

#### Journal of Environmental & Earth Sciences

https://journals.bilpubgroup.com/index.php/jees

#### ARTICLE

# Development of Multigeneration Waste-to-Zero System Using ORC, Sorption, and Drying-Based CCHP

Chanansith Suvarnabol 1,2, Nattaporn Chaiyat 1,2\*

#### **ABSTRACT**

This work investigates a combined cooling, heating, and power (CCHP) generation system utilizing waste energy. A cascade-CCHP system is developed, consisting of a 23.65-kWe organic Rankine cycle (ORC), a 4.00-kW adsorption chiller, a 4.11-kW absorption chiller, a 15.99-kW drying room, and an incinerator of 150 kg/h. A net energy production of 36.08 kWh is achieved from a CCHP energy efficiency of 9.98%. The levelized cost for producing a total energy output of 2,020,592 kWh over a lifespan of 20 years is approximately 0.106 USD/kWh. The life cycle assessment (LCA) yields a single score of approximately 0.000151 Pt, mainly attributed to raw materials used in the construction process of 87.16%. In addition, the combustion ash is processed into concrete blocks measuring 39 cm × 19 cm × 7 cm, in accordance with the Industrial Product Standard (TIS) 58-2533, with a water absorption value below 5% and a compressive strength exceeding 25 kg/cm2. The CCHP system demonstrates a novel method of waste-to-energy (WtE), and the construction material from waste combustion ash can also support a new concept of waste-to-zero (WtZ).

Keywords: Organic Rankine Cycle (ORC); Sorption System; Drying Room; Incinerator; Construction Material

#### \*CORRESPONDING AUTHOR:

Nattaporn Chaiyat, School of Renewable Energy, Maejo University, Chiang Mai 50290, Thailand; Thermal Design and Technology Laboratory (TDeT Lab), Chiang Mai 50290, Thailand; Email: benz178tii@hotmail.com

#### ARTICLE INFO

Received: 25 June 2025 | Revised: 5 August 2025 | Accepted: 7 August 2025 | Published Online: 19 August 2025 DOI: https://doi.org/10.30564/jees.v7i8.10712

#### CITATION

Suvarnabol, C., Chaiyat, N., 2025. Development of Multigeneration Waste-to-Zero System Using ORC, Sorption, and Drying-Based CCHP. Journal of Environmental & Earth Sciences. 7(8): 131–150. DOI: https://doi.org/10.30564/jees.v7i8.10712

#### COPYRIGHT

Copyright © 2025 by the author(s). Published by Bilingual Publishing Group. This is an open access article under the Creative Commons Attribution-NonCommercial 4.0 International (CC BY-NC 4.0) License (https://creativecommons.org/licenses/by-nc/4.0/).

<sup>&</sup>lt;sup>1</sup> School of Renewable Energy, Maejo University, Chiang Mai 50290, Thailand

<sup>&</sup>lt;sup>2</sup> Thermal Design and Technology Laboratory (TDeT Lab), Chiang Mai 50290, Thailand

## 1. Introduction

Thailand has long faced challenges in waste management. The government has implemented policies to support the conversion of waste-to-energy (WtE) for cooling, heating, and power generation systems. The National Energy Plan (NEP) 2024, issued by the Ministry of Energy, Thailand, sets target goals of 975-MW<sub>e</sub> of power and 495-ktoe of heat from waste energy [1]. A multigeneration system can enhance system efficiency in WtE energy technology. In addition, the issue of community waste management should be addressed locally, rather than relocating waste from its area of origin. Managing waste at the point of generation is considered a suitable solution for waste management in Thailand. On this basis, this work focuses on a combined WtE and waste-to-zero (WtZ) as a novel concept of waste-to-energy-to-zero (WtEtZ) for a sustainable approach to waste management in Thailand.

In recent works on multigeneration technology, Navaongxay and Chaiyat [2] studied the comparative efficiency improvement of an R-245fa ORC system combined with a water-lithium bromide (LiBr) absorption system. Their findings showed that replacing the ORC condenser with the absorption system resulted in an energy efficiency of 20.61% and an energy cost of 0.073 USD/kWh. This work follows a similar research approach to that of Cho et al. [3], who used a hybrid absorption chiller to improve energy efficiency, resulting in a 43% reduction in liquefied natural gas (LNG) consumption. Gimelli et al. [4] reported on an H<sub>2</sub>O-NH<sub>3</sub> (water-ammonia) absorption system integrated into a battery-supported combined cooling, heating, and power (CCHP) plant. The novel system demonstrated primary energy savings of 19.44% and a carbon dioxide (CO<sub>2</sub>) emissions reduction of 23.99%. In addition, Karim et al. [5] evaluated the energy and economic performance of the CCHP system for residential air conditioners. The results indicated that the ideal working fluid for the ORC unit is R-124, which could generate 4.25 kW<sub>e</sub> of electricity, 23.77 kW of heat, and 4.03 kW total energy production cost of 0.475 USD/h. Anvari materials. Carbonated ashes contained 0.3–35.3 g<sub>Carbon</sub>/

et al. [6] evaluated the energy, economic, and environmental (3E) aspects of the CCHP generation system from a water distillation system. The study found that the novel system produced 30.5 MW<sub>e</sub> of electricity, 40.8 MW of heat, 1 MW of cooling, and 0.364 kg/s of distilled water. The economic analysis showed a production cost of 1.909 USD/h. The environmental impact emitted 0.163 kg CO<sub>2</sub>-eq/kWh. Xu et al. [7] studied the optimal size of the generator in the CCHP system. The energy, economic, and environmental evaluation found that the multigeneration system had an energy efficiency of 68.79%, a fuel consumption rate of 209 kWh, a carbon dioxide emission rate of 26.82 kg CO<sub>2</sub>-eq/h, and a payback period of 3.21 years. The 3E optimization of the CCHP system was supported by Zhang [8], who developed a modified genetic algorithm (MGA) to investigate the performance of the CCHP system coupled with thermal energy storage (TES). Du et al. [9] presented a thermodynamic analysis of a copper-based chemical looping combustion system for the CCHP system. Thermal and energy efficiencies were found to be 72.34% and 40.54%, respectively. In the topic of WtE, Asim et al. [10] reported the 3E aspects of WtE potential in five populous cities of Pakistan. A 50-MW<sub>e</sub> WtE plant revealed a levelized cost of electricity (LCOE) of 7.86 ¢/kWh and greenhouse gas emissions of 216.6 million tons of CO<sub>2</sub>-eq over 25 years. Carneiro and Gomes [11] presented the waste-to-energy/gas turbine cycles. The hybrid system had a power output capacity of 107 MW<sub>e</sub>, a thermal efficiency of 36%, an ecological efficiency of 89%, and an LCOE of 64-89 US\$/MWh. The 3E model was commonly used to assess WtE by Tan et al. [12], who investigated suitable waste disposal methods, including landfill gas recovery systems, incineration, anaerobic digestion, and gasification in Malaysia. Bhuiyan et al. [13] analyzed the pyro-gasification of Norwegian industrial waste; Farajollahi et al. [14] reported on a biogas power plant for sustainable energy; and Ramos [15] investigated sustainable energy production from waste thermal conversion. In the management of waste ash, Cunningham et al. [16] of cooling, with an energy efficiency of 7.8% and a reported on carbonated biomass ashes for cementitious

kg<sub>Ash</sub>, resulting in an overall reduction in greenhouse heat production (points 1h-3h). The hot fluid is then gases (GHGs) emissions of less than 1% compared to untreated ashes. Incineration ash-to-cement studies were reported by Aouan et al. [17], who optimized the mechanical performance of fly ash-based geopolymer cement using artificial neural network modeling. Ramírez et al. [18] studied incineration ashes as building materials on San Andrés Island. Chen et al. [19] also developed municipal solid waste incinerator bottom ash as a construction material. The classified ash was studied to evaluate environmental safety and to avoid toxic elements. Zhou et al. [20] used 20% sintered incinerator fly ash with 1% alkali equivalent to enhance the properties of mortar for use in cementitious material. In addition, Schafer et al. [21] suggested blending incinerator bottom ash with natural aggregates as road base construction materials to reduce environmental concerns.

From the above research, the research gap of combined WtE and WtZ technologies has not been addressed. This study aims to implement a novel prototype of a multigeneration system for power (ORC), cooling (absorption and adsorption systems), and heating (drying room) processes using a small-scale incinerator, as well as to develop combustion ash into a construction material. The 3E analysis of energy, economic, and environmental impacts is conducted under the WtEtZ concept for sustainable waste management in Thailand. The objectives of this study are as follows:

- To develop and validate a multigeneration system using ORC, sorption cycles, and a drying unit capable of achieving above 8% energy efficiency.
- To convert 95% of combustion ash into environmentally safe construction blocks.
- · To study the energy, economic, and environmental (3E) impacts of the WtE production.

## 2. System Description

The novel multigeneration technology is shown in **Figure 1**. High-moisture waste is sent to a drying room to reduce its humidity and become waste fuel for comthe cogeneration incinerator include waste disposal and Table 1.

collected in a hot fluid tank (points 4h-9h). High-temperature hot water above 100 °C is supplied to an organic Rankine cycle power generation system, which transfers heat to an R-245fa working fluid (points 1–8). After that, the hot water decreases in temperature and is supplied to an adsorption cooling system (points 1d-6d). The working fluid (water) in the adsorption system evaporates from the adsorbent (silica gel) at evaporator number 1 to produce cold water (points 1cw-2cw). Then, the hot water is supplied to an absorption cooling system (points 1a-10a), where it transfers heat to the water-lithium bromide solution in evaporator number 2 to produce cold water (points 3cw-4cw). The hot water temperature is reduced and then used in the drying process (points 1DR-2DR). The multigeneration system in this research uses water cooling through a cooling tower (points 1c-12c).

The benefits of this research technology include the elimination of waste and the multigeneration of power, cooling, and heating. The combustion ash is used to produce concrete blocks for construction material. The highlights of this novel technology differ from those of general WtE systems, which can only produce power.

## 3. Materials and Methods

## 3.1. The Multigeneration Prototype

A novel multigeneration system consisting of an organic Rankine cycle with a maximum power generation capacity of 25 kW<sub>e</sub>, an adsorption cooling system with a maximum cooling capacity of 1.5 TR (5.28 kW), an absorption chiller of 1.5 TR, and a drying room with a maximum heating capacity of 20 kW. An incinerator with a maximum combustion rate of 200 kg/h and a hot-flow storage tank with a volume capacity of 2,000 L are used to support the hot fluid for the multigeneration system. A schematic diagram of the multigeneration prototype is illustrated in Figure 1. In addition, the specifications of bustion in a cogeneration incinerator. The benefits of each unit of the multigeneration system are represented in

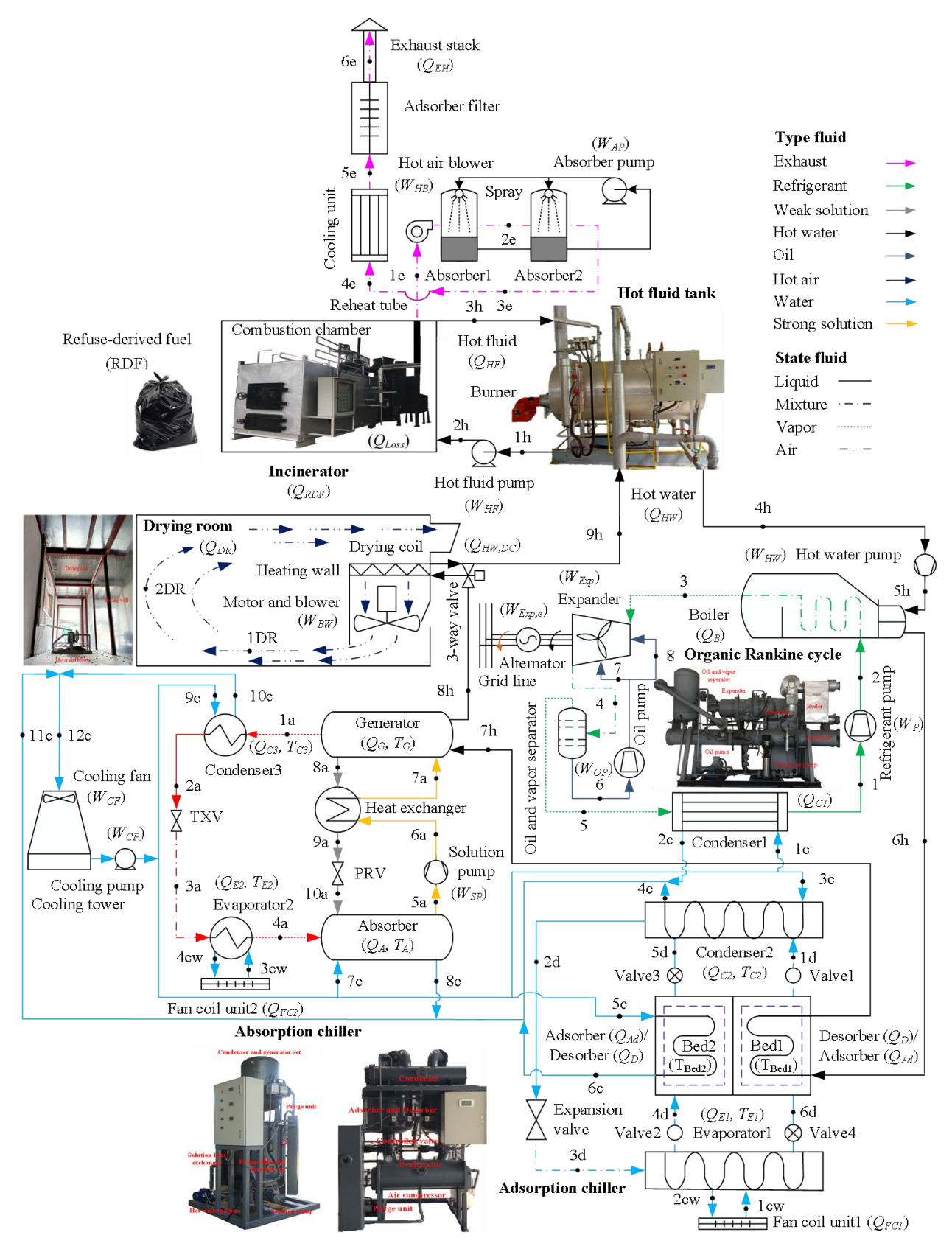


Figure 1. Simplified working diagram of the WtE technology.

#### **Table 1.** Specifications of the multigeneration prototype.

#### System

#### Description

#### Incinerator





- Combustion chamber volume 1.09 m<sup>3</sup>
- Heating capacity of double tube 250 kW
- Double absorber volume 1.147 m<sup>3</sup>/Unit
- Nozzle diameter 1 mm<sup>3</sup>
- Heating area of reheat tube 1.099 m<sup>2</sup>
- Heating area of cooling unit 1.815 m<sup>2</sup>
- Vacuum filter volume 0.157 m<sup>3</sup>
- Power consumption of hot air blower 1.50 kW<sub>e</sub>
- Power consumption of absorber pump 0.25 kW.

Hot fluid tank



- Maximum pressure 14 bar gauge
- Maximum volume capacity 1,500 L
- Volume flow rate 3.0-4.5 L/s
- Power consumption of hot fluid pump 2.2 kW.
- Power consumption of hot water pump 2.2 kW<sub>e</sub>

ORC

- Heating capacity of boiler 280 kW
- Mechanical power of double screw expander 30 kW
- Power generating of alternator 25 kW<sub>e</sub>
- Heating capacity of Condenser 250 kW
- · R-245fa as wording fluid
- Cooling capacity of cooling tower 80-TR
- Oil and vapor separator volume 60 L
- Power consumption of cooling pump 2.2 kW.
- Power consumption of cooling blower 1.2 kW<sub>e</sub>,
- Power consumption of oil pump 1.5 kW
- Power consumption of refrigerant pump 2.2 kW
- · Heating capacity of condenser 5.28 kW
- Heating capacity of adsorber and desorber 7.74 kW
- Heating capacity of Evaporator 5.28 kW
- Maximum pressure of air-compressor 700 kPa gauge
- Power consumption of air-compressor 0.55 kW
- Maximum pressure of butterfly valve actuator 1,000 kPa gauge
- Mass capacity of silica gel 25 kg/bed
- Specific resistance of silica gel  $\geq 4,000 \ \Omega \times cm$
- Density of silica gel 540 g/L
- Pore volume of silica gel 0.60–0.85 mL/g
- Pore diameter of silica gel 4.5–7.0 nm

Absorption chiller

Adsorption chiller



- Heating capacity of generator 8.28 kW
- Heating capacity of condenser 5.56 kW
- · Heating capacity of absorber 8.28 kW
- Heating capacity of evaporator 5.28 kW
- Heating capacity of solution heat exchanger 1.50 kW
- Power consumption of solution pump 0.37 kW<sub>e</sub>
- Water-lithium bromide as working pair
- Concentration of working pair 60–65% LiBr

Drying room



- Drying room sizing at width 3.6 m × length 6.0 m × height 2.5 m
- · Heating capacity of drying coil 20 kW
- Blower 4 blade
- Diameter of blower 20 inch
- Power consumption of motor 660 W<sub>e</sub>
- Speed of motor 1,440 rpm

## 3.2. Construction Material from Waste Combustion Ash

Environmentally friendly construction material made from waste combustion ash is developed in the form of concrete blocks. Standard tests for water absorption and compressive strength are conducted according to the Thai Industrial Standard (TIS) 58-2533.

### 3.3. Energy Impact Analysis

The energy efficiency of each cycle in the multigeneration system is analyzed using test results under steady-state conditions, as shown in Equations (1)–(5).

$$\eta_{ORC} = (W_{Exp,e} - W_{P,e} - W_{OP,e}) / Q_B \tag{1}$$

$$COP_{AD} = Q_E / Q_{De}$$
 (2)

$$COP_{AB} = Q_E / (Q_G + W_{SP}) \tag{3}$$

$$\eta_{DR} = Q_{Drying} / W_{Blowere} \tag{4}$$

$$\eta_{CCHP} = (W_{e,net} + Q_{Cooling} + Q_{Heating}) / Q_{HF}$$
 (5)

#### 3.4. Economic Evaluation

The levelized cost of energy (LCOE) for the multigeneration system using heat from waste combustion is analyzed. Total energy from power ( $W_{e,net}$ ), cooling ( $Q_{Cooling}$ ), and heating ( $Q_{Heating}$ ) is used to estimate the investment cost (Inv) and annual production cost (PEC), as shown in Equations (6) and (7).

$$LCOE = \frac{Inv + \sum_{t=1}^{N} \frac{PEC}{(1+r)^{t}}}{\sum_{t=1}^{N} \frac{(W_{e,net} + Q_{Cooling} + Q_{Heating})t_{OP}}{(1+DF)^{(t-1)}}}$$
(6)

$$r = ([1 + i_{\text{Real}}][1 + i_{\text{Inflation}}]) - 1 \tag{7}$$

## 3.5. Environmental Impact Assessment

The environmental impact assessment is conducted using the life cycle assessment (LCA) method in accordance with ISO 14040 and 14044 standards. The study scope is defined by a cradle-to-grave boundary with a system lifespan of 20 years. The LCA results are analyzed using the ReCiPe method and the SimaPro database [22]. Assessments of intermediate, final, and single-score impacts are performed, as shown in the assessment scope in **Figure 2**.

All eighteen midpoint and three endpoint impact categories of the ReCiPe method are are used to completely analyze the final impact score, as shown in Equations (8)–(14):

$$CV_i = CF_i x_i \tag{8}$$

$$CFm_{xc} = \sum CV_i \tag{9}$$

$$NP_i = CFm_{x,c} / NR_i t_{Pd} \tag{10}$$

$$WF_{i} = IP_{Reference\ vear,i} / IP_{Target\ vear,j}$$
 (11)

$$WP_i = WF_i NP_i \tag{12}$$

$$I_{m,Pd,Total} = \sum WP_{i} \tag{13}$$

$$I_{m.Pd.1 Unit} = \sum W P_i / \sum (W_{e.net} + Q_{Cooling} + Q_{Heating}) t_{OP} \quad (14)$$

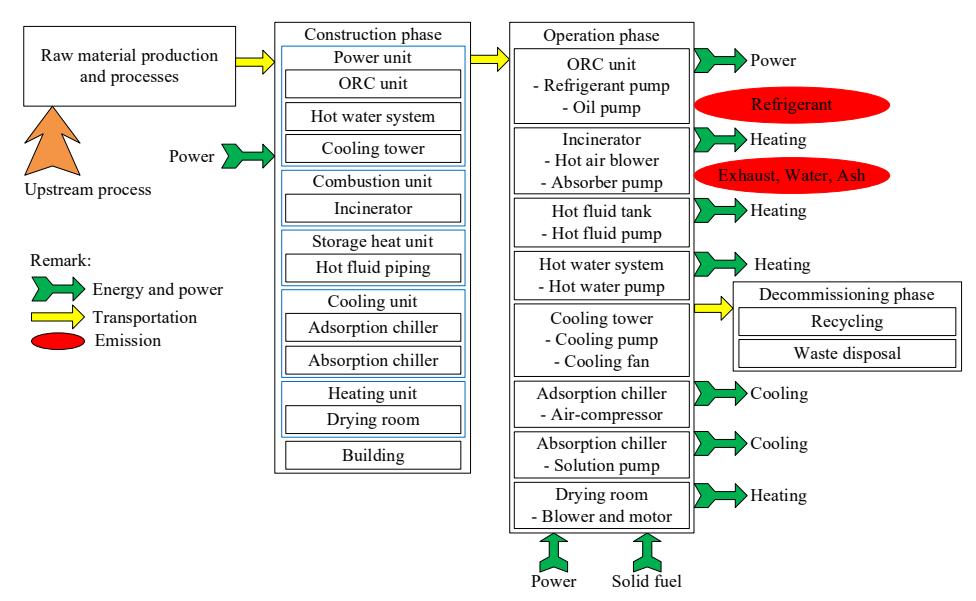


Figure 2. Scope and boundary conditions.

## 4. Results and Discussion

### 4.1. Energy Impact

The combustible waste, in the form of refuse-derived fuel type 3 (RDF-3), mainly consists of plastic waste with a mass flow rate ( $m_{RDF-3}$ ) of 92.21 kg/h and low heating value ( $LHV_{RDF-3}$ ) of 26.92 MJ/kg. The high heating value from dry waste, as presented in **Table 1**, conducts a supplied heat ( $Q_{RDF-3}$ ) of 689.15 kW. The hot fluid produced from waste heat recovery in the incinerator has inlet ( $T_{2h}$ ) and outlet ( $T_{3h}$ ) temperatures of approximately 90.43 °C and 106.06 °C, respectively; it can produce a hot fluid heating capacity ( $Q_{HF}$ ) of 361.39 kW. The electrical power consumption of the incinerator comes from an absorption pump ( $W_{AP}$ ) of 0.23 kW<sub>e</sub>, a hot fluid pump ( $W_{HF}$ ) of 1.89 kW<sub>e</sub>, and a hot air blower ( $W_{HB}$ ) of 1.31 kW<sub>e</sub>. Thus, the waste-to-heat incinerator has an energy efficiency ( $\eta_{ICH}$ ) of approximately 52.32%.

The hot water is then fed into the ORC system at a temperature  $(T_{5h})$  of approximately 105.37 °C. The working fluid (R-245fa) evaporates into vapor at a temperature  $(T_3)$  of 102.98 °C under a high-side pressure  $(P_{HORC})$  of 10.41 bar gauge. The hot water is then cooled and leaves the power generation system at a fluid temperature  $(T_{6h})$ of approximately 94.65 °C. Heat exchange occurs at the boiler  $(Q_B)$  with a capacity of 240.36 kW. The working fluid generates work at the expander  $(W_{Exp})$  of 44.61 kW and produces electricity from an alternator ( $W_{Exp,e}$ ) of 23.65 kW.. Meanwhile, the ORC system consumes electrical energy from a working fluid pump  $(W_{OP})$  of 1.4 kW<sub>e</sub> and a second pump  $(W_p)$  of 1.78 kW<sub>e</sub>, resulting in a net power generation ( $W_{ORC,net}$ ) of approximately 20.47 kW<sub>e</sub>. The heat-to-power process demonstrates an energy efficiency  $(n_{ORC})$  of 8.52%. This efficiency value is nearly that of a solar-biodiesel ORC system at 8.93% [23].

The adsorption refrigeration system converts heat into cooling. The working fluid (water) boils at a dual adsorber temperature ( $T_D = [T_{Bed1} + T_{Bed2}] / 2$ ) of 86.50 °C, derived from a hot water temperature ( $T_{Cow}$ ) of 94.65 °C. A cold water temperature ( $T_{Cow}$ ) of 10.48 °C is produced through heat transfer rates in the desorber ( $T_{Cow}$ ) of 7.73 kW, adsorbent ( $T_{Cow}$ ) of 7.53 kW, condenser ( $T_{Cow}$ ) of 4.63 kW, and evaporator ( $T_{Cow}$ ) of 4.00 kW. Power consumption occurs from the air compressor to control the solenoid valve ( $T_{Cow}$ ) at 0.046 kW<sub>e</sub>. As a result, the absorption chiller has

an adsorption coefficient of performance ( $COP_{AD}$ ) of 0.51. This efficiency value is nearly that of a solar-biodiesel adsorption chiller at 0.55 [23].

The absorption refrigeration system is used to operate the cooling process. The working fluid (water) boils at a generator temperature ( $T_G$ ) of 86.38 °C, with a heat transfer rate ( $Q_G$ ) of 7.72 kW from hot water at a temperature ( $T_{7h}$ ) of 94.07 °C; it can produce cold water at a temperature ( $T_{4cw}$ ) of 11.86 °C through heat transfer rates at the evaporator ( $Q_{E2}$ ) of 4.11 kW, the condenser ( $Q_{C3}$ ), and the absorber ( $Q_A$ ) of 7.66 kW. Power consumption from the solution pump ( $W_{SP}$ ) of 0.172 kW<sub>e</sub> affects the absorption coefficient of performance (COP<sub>AB</sub>), which is 0.52. This efficiency value is slightly lower than that of a solar-biodiesel absorption chiller at 0.74 [23]. A higher heat source temperature of 95 °C directly affects the better COP value.

The drying room is the final energy system of the multigeneration system. Hot water at a temperature  $(T_{8h})$  of 93.50 °C is supplied to the drying room to produce hot air at approximately 80 °C  $(T_{1DR})$ . This heat is used to reduce the moisture content of drying products to below 10% wet basis at a drying rate  $(Q_{DC})$  of 15.99 kW. Electrical power is supplied to a blower  $(W_{BW})$  of 0.60 kW<sub>e</sub>. The drying room has an energy efficiency  $(\eta_{DR})$  of approximately 40.54%. This efficiency value is nearly that of a geothermal drying room at 45.36%  $^{[24]}$ .

From the energy results of the multigeneration system, it was found that the cooling process of the absorption and desorption systems ( $E_{Cooling}$ ) is 8.11 kWh, the heating process from the drying room ( $E_{Heating}$ ) is 15.99 kWh, and the power process from the ORC system  $(E_{net,e})$ , after subtracting the electrical energy usage of all devices in the multigeneration system, is 11.98 kWh; these produce a total energy ( $E_{CCHP}$ ) of 36.08 kWh at an energy efficiency ( $\eta_{CCHP}$ ) of 9.98%, as shown in Figure 3 and Table 2. It was found that the multigeneration (power, cooling, and heating) system using waste fuel can increase energy production efficiency by approximately 37.05% compared to the waste-to-power (WtP) system, which has an energy efficiency  $(\eta_{WtP})$  of 7.29%. Although the CCHP efficiency of this work is lower than that of a geothermal-CCHP system at 11.62% [24]. A conversion efficiency of waste to heat fluid cycle of the incinerator is a disadvantage compared with a gasket plate

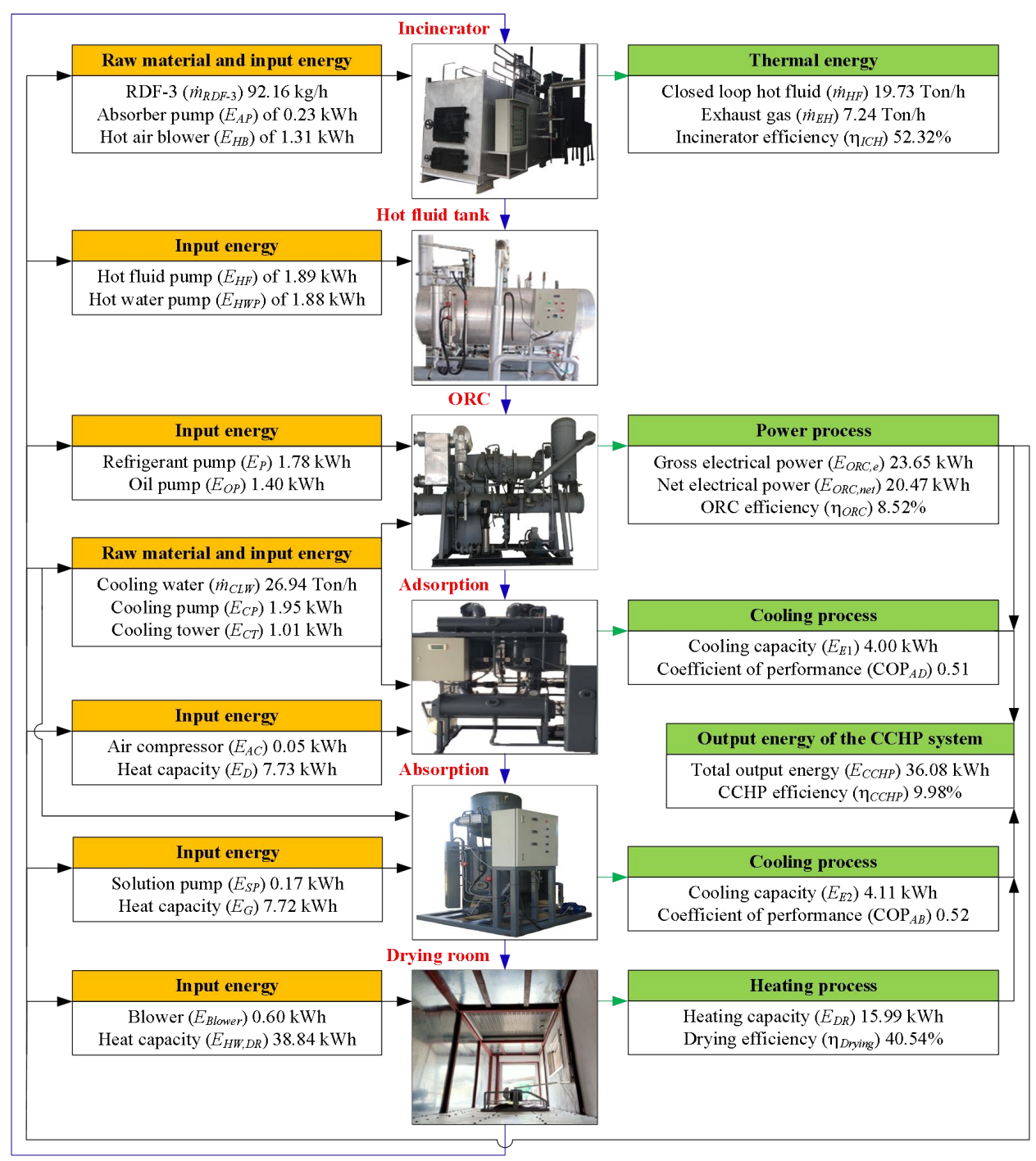


Figure 3. Energy yield of the WtE multigeneration system.

Table 2. Energy analysis results of the WtE multigeneration system.

Description	Value
RDF-3	
Moisture (MR <sub>Moisture</sub> , %wt)	5.65
$\overline{\mathrm{Ash}(MR_{Ash},\%\mathrm{wt})}$	6.45
Volatile matter (MR <sub>Volatile matter</sub> , %wt)	82.20
Fixed carbon $(MR_{Fixed\ carbon}, \%wt)$	5.70

Table 2. Cont.

Hydrogen (MR <sub>collaption</sub> Swort)         53.3           Carbon (MR <sub>Collaption</sub> Swort)         0.73           Nitrogen (MR <sub>collaption</sub> Swort)         25.35           Sulfur (MR <sub>collaption</sub> Swort)         0.14           High heating value (IHH <sub>BDC-15</sub> MJ/kg)         28.89           Low heating value (IHH <sub>BDC-15</sub> MJ/kg)         26.92           Incherator         The Mass flow rate of FbDF-3 ( $m_{BDC-15}$ kg/s)         0.0256           Mass flow rate of FbDF-3 ( $m_{BDC-15}$ kg/s)         5.48           Mass flow rate of crystall sign ( $m_{DC}$ kg/s)         5.48           Mass flow rate of crystall sign ( $m_{DC}$ kg/s)         5.48           Mass flow rate of crystall sign ( $m_{DC}$ kg/s)         5.48           Mass flow rate of crystall sign ( $m_{DC}$ kg/s)         5.48           Mass flow rate of crystall sign ( $m_{DC}$ kg/s)         5.48           Mass flow rate of crystall sign ( $m_{DC}$ kg/s)         5.48           Mass flow rate of Explain sign ( $m_{DC}$ kg/s)         5.48           Mass flow rate of crystall sign ( $m_{DC}$ kg/s)         5.48           Mass flow rate of Explain sign sign ( $m_{DC}$ kg/s)         5.48           Mass flow rate of Explain sign sign sign sign sign sign sign si	Description	Value
Nitrogen ( $MR_{Sungean}$ %wit)         0.73           Oxygen ( $MR_{Sungean}$ %wit)         25.35           Salibir ( $MR_{Sungean}$ %wit)         0.14           High heating value ( $HHF_{SDCA}$ , $MJAkg$ )         28.89           Low heating value ( $HHF_{SDCA}$ , $MJAkg$ )         26.92           Inchierator         ************************************	Hydrogen (MR <sub>Hydrogen</sub> , %wt)	9.33
Oxygen ( $MR_{Oxygen}$ %wit)         0.14           Sulfur ( $MR_{Super}$ %wit)         0.14           High heating value ( $HHP_{Birch}$ , MJ/kg)         28.89           Low heating value ( $HHP_{Birch}$ , MJ/kg)         26.92           Mass flow rate of RDF-3 ( $m_{Birch}$ , kg/s)         0.0256           Mass flow rate of both fluid ( $m_{ir}$ kg/s)         5.48           Mass flow rate of exhaust gas ( $m_{Birch}$ kg/s)         2.01           Hot fluid temperature leaving incinerator ( $T_{3i}$ °C')         106.07           Hot fluid temperature leaving incinerator ( $T_{3i}$ °C')         90.43           Estimation combustion temperature by color spectrometry technique ( $T_{Cip}$ °C')         1.200           Exhaust gas temperature leaving incinerator ( $T_{aic}$ °C')         22.56           Cooling water temperature entering absorber! ( $T_{Cip}$ °C')         28.56           The ambient temperature $T_{ci}$ °C')         31.7           Finality of hot fluid entering incinerator ( $h_{ia}$ , kJ/kg)         378.85           Enthalpy of the fluid entering incinerator ( $h_{ia}$ , kJ/kg)         472.35           Enthalpy of the ambient temperature ( $h_{ia}$ , kJ/kg)         472.35           Enthalpy of water entering absorber! ( $h_{ia}$ , kJ/kg)         472.35           Enthalpy of water entering absorber! ( $h_{ia}$ , kJ/kg)         119.71           Heating capacity of RDF ( $h_{ia}$ , kW) </td <td>Carbon (MR<sub>Carbon</sub>, %wt)</td> <td>58.00</td>	Carbon (MR <sub>Carbon</sub> , %wt)	58.00
Sulfur ( $MR_{caglow}$ %ww)         0.14           High beating value ( $HHV_{Biply}$ , MJ/kg)         28.89           Low heating value ( $HHV_{Biply}$ , MJ/kg)         26.92           Incinerator         The contract of RDF-3 ( $R_{Biply}$ , kg/s)         0.0256           Mass flow rate of RDF-3 ( $R_{Biply}$ , kg/s)         5.48           Mass flow rate of orb fluid ( $m_{Biply}$ , kg/s)         2.01           Hot fluid temperature entering incinerator ( $T_{2a}$ , °C)         106.07           Hot fluid temperature eleaving incinerator ( $T_{2a}$ , °C)         90.43           Estimation combustion temperature by color spectrometry technique ( $T_{C_{2b}}$ , °C)         1.200           Estimation combustion temperature by color spectrometry technique ( $T_{C_{2b}}$ , °C)         22.56           Cooling water temperature entering absorber ( $T_{C_{2c}}$ , °C)         28.56           The ambient temperature ( $T_{2a}$ , °C)         28.56           The ambient temperature ( $T_{2a}$ , °C)         31.7           Enthalpy of both fluid entering incinerator ( $R_{1a}$ , kJ/kg)         444.80           Enthalpy of both fluid entering incinerator ( $R_{1a}$ , kJ/kg)         472.35           Enthalpy of water entering absorber ( $R_{1a}$ , kJ/kg)         472.35           Enthalpy of water entering absorber ( $R_{1a}$ , kJ/kg)         119.71           Heating capacity of RDF ( $Q_{2a}$ , kW)         82.75 <tr< td=""><td>Nitrogen (MR<sub>Nitrogen</sub>, %wt)</td><td>0.73</td></tr<>	Nitrogen (MR <sub>Nitrogen</sub> , %wt)	0.73
High heating value ( $HHV_{SOF-3}$ , $MI/kg$ )         28.89           Low heating value ( $IHV_{SOF-3}$ , $MI/kg$ )         26.92           Incinerator         S           Mass flow rate of RDF-3 ( $m_{SOF-3}$ , $kg$ /s)         0.0256           Mass flow rate of bot fluid ( $m_{BP}$ , $kg$ /s)         5.48           Mass flow rate of exhaust gas ( $m_{DP}$ , $kg$ /s)         2.01           Hot fluid temperature leaving incinerator ( $T_{2a}$ , ${}^{*}$ C)         106.07           Hot fluid temperature leaving incinerator ( $T_{DP}$ , ${}^{*}$ C)         90.43           Estimation combustion temperature value (aving incinerator ( $T_{CP}$ , ${}^{*}$ C)         12.00           Exhaust gas temperature leaving incinerator ( $T_{CP}$ , ${}^{*}$ C)         28.56           Cooling water temperature entering absorber ( $T_{CPP}$ , ${}^{*}$ C)         31.7           Enthalpy of hot fluid elerting incinerator ( $h_{BS}$ , $kJkg$ )         444.80           Enthalpy of hot fluid elerting incinerator ( $h_{BS}$ , $kJkg$ )         378.85           Enthalpy of water entering absorber ( $M_{CPD}$ , $kJkg$ )         431.18           Enthalpy of water entering absorber ( $M_{CPD}$ , $kJkg$ )         431.18           Enthalpy of water entering absorber ( $M_{CPD}$ , $kJkg$ )         431.18           Enthalpy of water entering absorber ( $M_{CPD}$ , $kJkg$ )         431.18           Enthalpy of water entering absorber ( $M_{CPD}$ , $kJkg$ )         431.39	Oxygen (MR <sub>Oxygen</sub> , %wt)	25.35
Low heating value ( $LHV_{RDS-3}$ , $MJ/kg$ )         26.92           Incinerator         Name of RDF-3 ( $n_{RDS-3}$ , $kg/s$ )         0.0256           Mass flow rate of RDF-3 ( $n_{RDS-3}$ , $kg/s$ )         5.48           Mass flow rate of exhaust gas ( $n_{RD}$ , $kg/s$ )         2.01           Hot fluid temperature entering incinerator ( $T_{20}$ , ${}^{\circ}$ C)         106.07           Hot fluid temperature leaving incinerator ( $T_{20}$ , ${}^{\circ}$ C)         90.43           Estimation combustion temperature by color spectrometry technique ( $T_{CB}$ , ${}^{\circ}$ C)         12.00           Exhaust gas temperature leaving incinerator ( $T_{20}$ , ${}^{\circ}$ C)         72.56           Cooling water temperature entering absorber! ( $T_{CB}$ , ${}^{\circ}$ C)         28.56           The ambient temperature ( $T_{20}$ , ${}^{\circ}$ C)         31.7           Enthalpy of both fluid entering incinerator ( $h_{30}$ , $kJ/kg$ )         444.80           Enthalpy of both fluid leaving incinerator ( $h_{30}$ , $kJ/kg$ )         472.35           Enthalpy of the fluid leaving incinerator ( $h_{30}$ , $kJ/kg$ )         472.35           Enthalpy of the subset temperature ( $h_{30}$ , $kJ/kg$ )         472.35           Enthalpy of water entering absorber! ( $h_{20}$ , $kJ/kg$ )         472.35           Enthalpy of water entering absorber! ( $h_{20}$ , $kJ/kg$ )         472.35           Heating capacity of RDF ( $Q_{20}$ , $kW$ )         82.75	Sulfur (MR <sub>Sulfur</sub> , %wt)	0.14
Incinerator         Mass flow rate of RDF-3 ( $m_{BDP-3}$ , $k_B/s$ )         0.0256           Mass flow rate of ch fluid ( $m_{BP}$ , $k_B/s$ )         5.48           Mass flow rate of cheshaust gas ( $m_{BD}$ , $k_B/s$ )         2.01           Hot fluid temperature entering incinerator ( $T_{2a}$ , ${}^{c}$ C)         106.07           Hot fluid temperature leaving incinerator ( $T_{a_0}$ , ${}^{c}$ C)         90.43           Estimation combustion temperature by color spectrometry technique ( $T_{CD}$ , ${}^{c}$ C)         72.56           Cooling water temperature leaving incinerator ( $T_{a_0}$ , ${}^{c}$ C)         28.56           The ambient temperature entering absorber1 ( $T_{CD}$ , ${}^{c}$ C)         31.7           Enthalpy of hot fluid entering incinerator ( $h_{2a}$ , $kJ/kg$ )         444.80           Enthalpy of bot fluid leaving incinerator ( $h_{2a}$ , $kJ/kg$ )         378.85           Enthalpy of the ambient temperature ( $h_{CD}$ , $kJ/kg$ )         431.18           Enthalpy of water entering absorber1 ( $h_{CD}$ , $kJ/kg$ )         431.18           Enthalpy of water entering absorber1 ( $h_{CD}$ , $kJ/kg$ )         119.71           Heating capacity of RDF ( $Q_{DPC}$ -3, $kJ$ )         689.15           Heating capacity of bot fluid ( $Q_{DPC}$ -3, $kJ$ )         82.75           Heating capacity of bot fluid ( $Q_{DPC}$ -3, $kJ$ )         689.15           Heating capacity of bot fluid ( $Q_{DPC}$ -3, $kJ$ )         689.15	High heating value (HHV <sub>RDF-3</sub> , MJ/kg)	28.89
Mass flow rate of RDF-3 ( $m_{ROP,T}$ , kg/s)       5.48         Mass flow rate of hot fluid ( $m_{RO}$ , kg/s)       5.48         Mass flow rate of hot fluid ( $m_{RO}$ , kg/s)       2.01         Hot fluid temperature entering incinerator ( $T_{2a}$ , °C)       106.07         Hot fluid temperature leaving incinerator ( $T_{2a}$ , °C)       99.43         Estimation combustion temperature by color spectrometry technique ( $T_{CD}$ , °C)       72.56         Exhaust gas temperature leaving incinerator ( $T_{aa}$ , °C)       72.56         Cooling water temperature entering absorber! ( $T_{CE}$ , °C)       28.56         The ambient temperature ( $T_{aa}$ , °C)       31.7         Enthalpy of hot fluid entering incinerator ( $h_{ab}$ , kJ/kg)       444.80         Enthalpy of the fluid entering incinerator ( $h_{ba}$ , kJ/kg)       378.85         Enthalpy of the ambient temperature ( $h_{ba}$ , kJ/kg)       378.85         Enthalpy of the ambient temperature ( $h_{ba}$ , kJ/kg)       431.18         Enthalpy of water entering absorber! ( $h_{ce}$ , kJ/kg)       431.18         Enthalpy of water entering absorber! ( $h_{ce}$ , kJ/kg)       19.71         Heating capacity of RDF ( $Q_{2ap}$ , kW)       689.15         Heating capacity of schaust gas ( $Q_{ce}$ , kW)       361.39         Heat loss at incinerator ( $Q_{ce}$ , kW)       36.39         Power consumption of hot air blower ( $W_{in}$ , kW) <t< td=""><td>Low heating value (<math>LHV_{RDF-3}</math>, MJ/kg)</td><td>26.92</td></t<>	Low heating value ( $LHV_{RDF-3}$ , MJ/kg)	26.92
Mass flow rate of hot fluid ( $m_{BP}$ , kg/s)       5.48         Mass flow rate of exhaust gas ( $n_{EB}$ , kg/s)       2.01         Hot fluid temperature entering incinerator ( $T_{2a}$ , °C)       106.07         Hot fluid temperature leaving incinerator ( $T_{2a}$ , °C)       99.43         Estimation combustion temperature by color spectrometry technique ( $T_{CB}$ , °C)       1.200         Exhaust gas temperature leaving incinerator ( $T_{6a}$ , °C)       72.56         Cooling water temperature cutering absorber! ( $T_{CB}$ , °C)       28.56         The ambient temperature ( $T_{9}$ , °C)       31.7         Enthalpy of hot fluid entering incinerator ( $h_{5a}$ , kJ/kg)       444.80         Enthalpy of hot fluid entering incinerator ( $h_{6a}$ , kJ/kg)       378.85         Enthalpy of hot fluid leaving incinerator ( $h_{6a}$ , kJ/kg)       472.35         Enthalpy of hot fluid leaving incinerator ( $h_{6a}$ , kJ/kg)       472.35         Enthalpy of the ambient temperature ( $h_{6a}$ , kJ/kg)       472.35         Enthalpy of the ambient temperature ( $h_{6a}$ , kJ/kg)       471.18         Enthalpy of water entering absorber! ( $h_{CB}$ , kJ/kg)       481.18         Enthalpy of water entering absorber! ( $h_{CB}$ , kJ/kg)       189.19         Heating capacity of RDF ( $Q_{2as}$ , kW)       82.75         Heating capacity of the fluid ( $Q_{BB}$ , kW)       82.75         Heating capacity of hot flu	Incinerator	
Mass flow rate of exhaust gas ( $m_{EP}$ , $k_F$ /s)       2.01         Hot fluid temperature entering incinerator ( $T_{2a}$ , °C)       106.07         Hot fluid temperature leaving incinerator ( $T_{3a}$ , °C)       90.43         Estimation combustion temperature by color spectrometry technique ( $T_{CD}$ , °C)       1,200         Exhaust gas temperature leaving incinerator ( $T_{ac}$ , °C)       72.56         Cooling water temperature entering absorber1 ( $T_{CEP}$ , °C)       28.56         The ambient temperature ( $T_a$ , °C)       31.7         Enthalpy of hot fluid entering incinerator ( $h_{2a}$ , $kJk/kg$ )       444.80         Enthalpy of hot fluid leaving incinerator ( $h_{ab}$ , $kJ/kg$ )       378.85         Enthalpy of thot fluid leaving incinerator ( $h_{ab}$ , $kJ/kg$ )       431.18         Enthalpy of thot fluid leaving incinerator ( $h_{ab}$ , $kJ/kg$ )       431.18         Enthalpy of the ambient temperature ( $h_a$ , $kJ/kg$ )       431.18         Enthalpy of water entering absorber1 ( $h_{cR/k}$ , $kJ/kg$ )       119.71         Heating capacity of RDF ( $Q_{abs-2a}$ , $kW$ )       689.15         Heating capacity of Post ( $Q_{abs-2a}$ , $kW$ )       82.75         Heating capacity of hot fluid ( $Q_{abs}$ , $kW$ )       361.39         Heat loss at incinerator ( $Q_{abs-2a}$ , $kW$ )       245.01         Power consumption of bot air blower ( $W_{abs-2a}$ , $kW_a$ )       1.31         Energy	Mass flow rate of RDF-3 ( $\dot{m}_{RDF-3}$ , kg/s)	0.0256
Hot fluid temperature entering incinerator ( $T_{2a}$ , °C) 90.43  Estimation combustion temperature by color spectrometry technique ( $T_{CB}$ , °C) 1,200  Exhaust gas temperature leaving incinerator ( $T_{aa}$ , °C) 72.56  Cooling water temperature entering absorber1 ( $T_{CW}$ , °C) 28.56  The ambient temperature $T_{CB}$ , °C) 31.7  Enthalpy of hot fluid entering incinerator ( $T_{ba}$ , $T_{ba}$ , $T_{ba}$ ) 444.80  Enthalpy of hot fluid entering incinerator ( $T_{ba}$ , $T_{ba}$ , $T_{ba}$ ) 444.80  Enthalpy of the thin ideaving incinerator ( $T_{ba}$ , $T_{ba}$ , $T_{ba}$ ) 472.35  Enthalpy of the mabient temperature ( $T_{ba}$ , $T_{ba}$ , $T_{ba}$ ) 472.35  Enthalpy of the ambient temperature ( $T_{ba}$ , $T_{ba}$ , $T_{ba}$ ) 472.35  Enthalpy of water entering absorber1 ( $T_{CW}$ , $T_{ba}$ ) 431.18  Enthalpy of water entering absorber1 ( $T_{CW}$ , $T_{ba}$ ) 431.18  Enthalpy of water entering absorber1 ( $T_{CW}$ , $T_{ba}$ ) 431.18  Enthalpy of water ontering absorber1 ( $T_{CW}$ , $T_{ba}$ ) 431.18  Enthalpy of schaust gas ( $T_{DM}$ , $T_{ba}$ ) 482.75  Heating capacity of RDF ( $T_{DM}$ , $T_{ba}$ ) 482.75  Heating capacity of hot fluid ( $T_{DW}$ , $T_{ba}$ ) 482.75  Heating capacity of hot fluid ( $T_{DW}$ , $T_{ba}$ ) 482.71  Power consumption of hot air blower ( $T_{DW}$ , $T_{ba}$ ) 482.71  Power consumption of hot air blower ( $T_{DW}$ , $T_{ba}$ ) 482.71  Energy efficiency of incinerator ( $T_{DW}$ , $T_{ba}$ ) 483.8  High-side pressure ( $T_{DW}$ , $T_{ba}$ ) 485.  Hower consumption of hot water pump ( $T_{DW}$ , $T_{ba}$ ) 485.  High-side pressure ( $T_{DW}$ , $T_{ba}$ ) 485.  High-side pressure ( $T_{DW}$ , $T_{ba}$ ) 486.  High-side pressure ( $T_{DW$	Mass flow rate of hot fluid ( $\dot{m}_{HF}$ , kg/s)	5.48
Hot fluid temperature leaving incinerator ( $T_{\rm Sh}$ °C) 90.43  Estimation combustion temperature by color spectrometry technique ( $T_{\rm CB}$ °C) 1,200  Exhaust gas temperature leaving incinerator ( $T_{\rm fe}$ °C) 72.56  Cooling water temperature entering absorber1 ( $T_{\rm CBF}$ °C) 28.56  The ambient temperature ( $T_{\rm o}$ °C) 31.7  Enthalpy of hot fluid entering incinerator ( $h_{2h}$ , $kJ/kg$ ) 444.80  Enthalpy of hot fluid leaving incinerator ( $h_{2h}$ , $kJ/kg$ ) 378.85  Enthalpy of the fluid leaving incinerator ( $h_{ab}$ , $kJ/kg$ ) 472.35  Enthalpy of exhaust entering incinerator ( $h_{ab}$ , $kJ/kg$ ) 472.35  Enthalpy of water entering absorber1 ( $h_{CRF}$ , $kJ/kg$ ) 471.18  Enthalpy of water entering absorber1 ( $h_{CRF}$ , $kJ/kg$ ) 119.71  Heating capacity of $P_{CRF}$	Mass flow rate of exhaust gas ( $\dot{m}_{EH}$ , kg/s)	2.01
Estimation combustion temperature by color spectrometry technique $(T_{CB}, {}^{\circ}C)$ 1,200  Exhaust gas temperature leaving incinerator $(T_{CB}, {}^{\circ}C)$ 22.56  Cooling water temperature entering absorber1 $(T_{CWD}, {}^{\circ}C)$ 31.7  The ambient temperature $(T_B, {}^{\circ}C)$ 31.7  Enthalpy of hot fluid entering incinerator $(h_{3a}, kJ/kg)$ 378.85  Enthalpy of bot fluid leaving incinerator $(h_{3a}, kJ/kg)$ 378.85  Enthalpy of exhaust entering incinerator $(h_{aa}, kJ/kg)$ 441.18  Enthalpy of water entering absorber1 $(h_{CWD}, kJ/kg)$ 431.18  Enthalpy of water entering absorber1 $(h_{CWD}, kJ/kg)$ 119.71  Heating capacity of RDF $(Q_{DDP-D}, kW)$ 689.15  Heating capacity of exhaust gas $(Q_{EB}, kW)$ 361.39  Heat loss at incinerator $(Q_{Loss}, kW)$ 361.39  Heat loss at incinerator $(Q_{Loss}, kW)$ 245.01  Power consumption of absorber pump $(W_{LD}, kW_0)$ 0.23  Power consumption of hot air blower $(W_{RD}, kW_0)$ 0.23  Hot fluid tank  Power consumption of hot fluid pump $(W_{RD}, kW_0)$ 1.89  Power consumption of hot water pump $(W_{LD}, kW_0)$ 1.89  Power consumption of hot water pump $(W_{RD}, kW_0)$ 1.89  Hower consumption of hot water pump $(W_{RD}, kW_0)$ 1.89  Power consumption of hot water pump $(W_{RD}, kW_0)$ 1.89  Power consumption of hot of the gauge) 0.97  ORC  Hot water temperature entering ORC $(T_{Sa}, {}^{\circ}C)$ 105.38  Hot water temperature leaving ORC $(T_{Sa}, {}^{\circ}C)$ 34.65  High-side pressure $(P_{R,DRC}, bar gauge)$ 1.70  Power consumption of oil pump $(W_{CD}, kW_0)$ 1.78  Power consumption of working fluid pump $(W_{CD}, kW_0)$ 1.95  Power consumption of working fluid pump $(W_{CD}, kW_0)$ 1.95  Power consumption of cooling pump $(W_{CD}, kW_0)$ 1.95	Hot fluid temperature entering incinerator $(T_{2h}, {}^{\circ}C)$	106.07
Exhaust gas temperature leaving incinerator $(T_{k_0}, {}^{\circ}C)$ 72.56  Cooling water temperature entering absorber1 $(T_{CW,0}, {}^{\circ}C)$ 31.7  Enthalpy of hot fluid entering incinerator $(h_{3a}, kJ/kg)$ 444.80  Enthalpy of hot fluid leaving incinerator $(h_{3a}, kJ/kg)$ 378.85  Enthalpy of exhaust entering incinerator $(h_{6a}, kJ/kg)$ 472.35  Enthalpy of the ambient temperature $(h_{CW,0}, kJ/kg)$ 431.18  Enthalpy of water entering absorber1 $(h_{CW,0}, kJ/kg)$ 431.18  Enthalpy of water entering absorber1 $(h_{CW,0}, kJ/kg)$ 119.71  Heating capacity of RDF $(Q_{RDF,0}, kW)$ 689.15  Heating capacity of the fluid $(Q_{RF}, kW)$ 361.39  Heat loss at incinerator $(Q_{Luo}, kW)$ 361.39  Heat loss at incinerator $(Q_{Luo}, kW)$ 245.01  Power consumption of absorber pump $(W_{AF}, kW_0)$ 0.23  Power consumption of hot air blower $(W_{RB}, kW_0)$ 1.31  Energy efficiency of incinerator $(\eta_{KF}, kW)$ 1.89  Power consumption of hot fluid pump $(W_{RF}, kW_0)$ 1.89  Power consumption of hot water pump $(W_{RF}, kW_0)$ 1.89  Power consumption of hot water pump $(W_{RF}, kW_0)$ 1.89  Power consumption of hot water pump $(W_{RF}, kW_0)$ 1.89  Hot fluid tank  Power consumption of hot water pump $(W_{RF}, kW_0)$ 1.89  Power consumption of hot water pump $(W_{RF}, kW_0)$ 1.89  Hot water temperature entering ORC $(T_{3a}, {}^{\circ}C)$ 105.38  Hot water temperature leaving ORC $(T_{3a}, {}^{\circ}C)$ 105.38  Hot water temperature leaving ORC $(T_{3a}, {}^{\circ}C)$ 10.41  Low-side pressure $(P_{LORC}, bar gauge)$ 1.70  Power consumption of oil pump $(W_{CF}, kW_0)$ 1.78  Power consumption of working fluid pump $(W_{CF}, kW_0)$ 1.78  Power consumption of cooling pump $(W_{CF}, kW_0)$ 1.79  Power consumption of cooling pump $(W_{CF}, kW_0)$ 1.79  Power consumption of cooling pump $(W_{CF}, kW_0)$ 1.95  Power consumption of cooling pump $(W_{CF}, kW_0)$ 1.95  Power consumption of cooling pump $(W_{CF}, kW_0)$ 1.95	Hot fluid temperature leaving incinerator $(T_{3h}, {}^{\circ}\text{C})$	90.43
Cooling water temperature entering absorber ( $T_{CW,P}$ , °C)       28.56         The ambient temperature ( $T_{O}$ , °C)       31.7         Enthalpy of hot fluid entering incinerator ( $h_{20}$ , $kJ/kg$ )       444.80         Enthalpy of hot fluid leaving incinerator ( $h_{30}$ , $kJ/kg$ )       378.85         Enthalpy of exhaust entering incinerator ( $h_{60}$ , $kJ/kg$ )       431.18         Enthalpy of the ambient temperature ( $h_{00}$ , $kJ/kg$ )       431.18         Enthalpy of water entering absorber ( $h_{CW,0}$ , $kJ/kg$ )       119.71         Heating capacity of RDF ( $Q_{RDF-3}$ , kW)       689.15         Heating capacity of exhaust gas ( $Q_{ED}$ , kW)       82.75         Heating capacity of tot fluid ( $Q_{BD}$ , kW)       361.39         Heat loss at incinerator ( $Q_{LOW}$ , kW)       245.01         Power consumption of absorber pump ( $W_{AP}$ , kW <sub>2</sub> )       0.23         Power consumption of hot air blower ( $W_{AP}$ , kW <sub>2</sub> )       1.31         Energy efficiency of incinerator ( $\eta_{ACP}$ , %)       52.32         Hot fluid tank       1.89         Power consumption of hot thuid pump ( $W_{AP}$ , kW <sub>2</sub> )       1.89         Power consumption of hot water pump ( $W_{AP}$ , kW <sub>2</sub> )       1.89         Power consumption of hot water pump ( $W_{AP}$ , kW <sub>2</sub> )       1.95         Hot water temperature entering ORC ( $T_{30}$ , °C)       105.38         Hot water t	Estimation combustion temperature by color spectrometry technique $(T_{CB}, {}^{\circ}C)$	1,200
The ambient temperature ( $T_{o_1}$ °C)       31.7         Enthalpy of hot fluid entering incinerator ( $h_{2a}$ , kJ/kg)       444.80         Enthalpy of bot fluid leaving incinerator ( $h_{2a}$ , kJ/kg)       378.85         Enthalpy of exhaust entering incinerator ( $h_{6c}$ , kJ/kg)       472.35         Enthalpy of the ambient temperature ( $h_{0c}$ , kJ/kg)       431.18         Enthalpy of water entering absorber1 ( $h_{CR/c}$ , kJ/kg)       119.71         Heating capacity of RDF ( $Q_{RDE,D}$ , kW)       689.15         Heating capacity of exhaust gas ( $Q_{ER/c}$ , kW)       82.75         Heating capacity of hot fluid ( $Q_{BR}$ , kW)       361.39         Heating capacity of hot fluid ( $Q_{BR}$ , kW)       361.39         Heat loss at incinerator ( $Q_{Lon}$ , kW)       245.01         Power consumption of absorber pump ( $W_{AR}$ , kW <sub>c</sub> )       0.23         Power consumption of hot air blower ( $W_{BR}$ , kW <sub>c</sub> )       1.31         Energy efficiency of incinerator ( $η_{ECR}$ , %)       52.32         Hot fluid tank       1.89         Power consumption of hot fluid pump ( $W_{BR}$ , kW <sub>c</sub> )       1.88         High-side pressure ( $P_{HJRT}$ , bar gauge)       0.97         ORC       105.38         Hot water temperature entering ORC ( $T_{ab}$ , °C)       105.38         Hot water temperature leaving ORC ( $T_{ab}$ , °C)       10.41      <	Exhaust gas temperature leaving incinerator $(T_{6e}, {}^{\circ}C)$	72.56
Enthalpy of hot fluid entering incinerator $(h_{2h}, kJ/kg)$ 378.85  Enthalpy of hot fluid leaving incinerator $(h_{1h}, kJ/kg)$ 378.85  Enthalpy of exhaust entering incinerator $(h_{6h}, kJ/kg)$ 472.35  Enthalpy of the ambient temperature $(h_{6h}, kJ/kg)$ 431.18  Enthalpy of water entering absorber1 $(h_{CW,h}, kJ/kg)$ 119.71  Heating capacity of RDF $(Q_{BDF,h}, kW)$ 689.15  Heating capacity of exhaust gas $(Q_{EH}, kW)$ 361.39  Heating capacity of the fluid $(Q_{HF}, kW)$ 361.39  Heat loss at incinerator $(Q_{Los}, kW)$ 245.01  Power consumption of absorber pump $(W_{AF}, kW_c)$ 0.23  Power consumption of hot air blower $(W_{BF}, kW_c)$ 32.32  Hot fluid tank  Power consumption of hot fluid pump $(W_{HF}, kW_c)$ 1.89  Power consumption of hot water pump $(W_{HF}, kW_c)$ 1.88  High-side pressure $(P_{BJFT}, \text{ bar gauge})$ 0.97  ORC  Hot water temperature entering ORC $(T_{5h}, {}^{\circ}C)$ 105.38  Hot water temperature leaving ORC $(T_{5h}, {}^{\circ}C)$ 34.65  High-side pressure $(P_{BJFT}, \text{ bar gauge})$ 1.70  Power consumption of oil working fluid pump $(W_{FF}, kW_c)$ 1.78  Power consumption of of working fluid pump $(W_{FF}, kW_c)$ 1.79  Power consumption of of oroling pump $(W_{CF}, kW_c)$ 1.95  Power consumption of cooling pump $(W_{CF}, kW_c)$ 1.95  Power consumption of cooling pump $(W_{CF}, kW_c)$ 1.97  Power consumption of cooling pump $(W_{CF}, kW_c)$ 1.99  Power consumption of cooling pump $(W_{CF}, kW_c)$ 1.91  Power consumption of cooling pump $(W_{CF}, kW_c)$ 1.95  Power consumption of cooling pump $(W_{CF}, kW_c)$ 1.91  Power consumption of cooling pump $(W_{CF}, kW_c)$ 1.91  Power consumption of cooling pump $(W_{CF}, kW_c)$ 1.91  Power of expander $(W_{E\psi}, kW_c)$ 44.61	Cooling water temperature entering absorber1 ( $T_{CW,i}$ , °C)	28.56
Enthalpy of hot fluid leaving incinerator $(h_{3a}, kJ/kg)$ 378.85  Enthalpy of exhaust entering incinerator $(h_{6c}, kJ/kg)$ 472.35  Enthalpy of the ambient temperature $(h_{6c}, kJ/kg)$ 431.18  Enthalpy of water entering absorber $(h_{CR/b}, kJ/kg)$ 119.71  Heating capacity of RDF $(Q_{RDF,b}, kW)$ 689.15  Heating capacity of exhaust gas $(Q_{EIR}, kW)$ 82.75  Heating capacity of hot fluid $(Q_{IIS}, kW)$ 361.39  Heat loss at incinerator $(Q_{Los}, kW)$ 245.01  Power consumption of absorber pump $(W_{AIP}, kW_c)$ 0.23  Power consumption of hot air blower $(W_{IIB}, kW_c)$ 1.31  Energy efficiency of incinerator $(\eta_{CIR}, \%)$ 52.32  Hot fluid tank  Power consumption of hot fluid pump $(W_{IIS}, kW_c)$ 1.89  Power consumption of hot water pump $(W_{III}, kW_c)$ 1.88  High-side pressure $(P_{ILIIIT})$ bar gauge) 0.97  ORC  Hot water temperature entering ORC $(T_{5a}, {}^{\circ}C)$ 105.38  Hot water temperature leaving ORC $(T_{5a}, {}^{\circ}C)$ 94.65  High-side pressure $(P_{ILIIIT})$ bar gauge) 1.70  Power consumption of oil pump $(W_{IIP}, kW_c)$ 1.4  Power consumption of working fluid pump $(W_{PP}, kW_c)$ 1.78  Power consumption of cooling pump $(W_{CP}, kW_c)$ 1.95  Power consumption of cooling pump $(W_{CP}, kW_c)$ 1.95  Power consumption of cooling tower $(W_{CP}, kW_c)$ 1.97  Power consumption of cooling tower $(W_{CP}, kW_c)$ 1.99  Power consumption of cooling tower $(W_{CP}, kW_c)$ 1.90	The ambient temperature $(T_0, {}^{\circ}C)$	31.7
Enthalpy of exhaust entering incinerator ( $h_{oc}$ , kJ/kg)472.35Enthalpy of the ambient temperature ( $h_{oc}$ , kJ/kg)431.18Enthalpy of water entering absorber1 ( $h_{CW_o}$ , kJ/kg)119.71Heating capacity of RDF ( $Q_{RDF-3}$ , kW)689.15Heating capacity of exhaust gas ( $Q_{Eib}$ , kW)82.75Heating capacity of hot fluid ( $Q_{Im}$ , kW)361.39Heat loss at incinerator ( $Q_{Los}$ , kW)245.01Power consumption of absorber pump ( $W_{AP}$ , kW $_{e}$ )0.23Power consumption of hot air blower ( $W_{IIB}$ , kW $_{e}$ )1.31Energy efficiency of incinerator ( $\eta_{ICID}$ , %)52.32Hot fluid tank $N_{Eight}$ Power consumption of hot taltid pump ( $W_{IIP}$ , kW $_{e}$ )1.88High-side pressure ( $P_{ILIRIT}$ ) bar gauge)0.97ORC105.38Hot water temperature entering ORC ( $T_{Sh}$ , °C)94.65High-side pressure ( $P_{ILIRIT}$ ) bar gauge)10.41Low-side pressure ( $P_{ILIRIT}$ ) bar gauge)10.41Low-side pressure ( $P_{ILIRIT}$ ) bar gauge)1.70Power consumption of oil pump ( $W_{OP}$ , kW $_{e}$ )1.4Power consumption of working fluid pump ( $W_{Pr}$ , kW $_{e}$ )1.78Power consumption of cooling pump ( $W_{CP}$ , kW $_{e}$ )1.95Power consumption of cooling tower ( $W_{CP}$ , kW $_{e}$ )1.01Power of expander ( $W_{Esp}$ , kW)44.61	Enthalpy of hot fluid entering incinerator $(h_{2h}, kJ/kg)$	444.80
Enthalpy of the ambient temperature $(h_0, kl/kg)$ 431.18Enthalpy of water entering absorber1 $(h_{CW,r}, kl/kg)$ 119.71Heating capacity of RDF $(Q_{RDF,S}, kW)$ 689.15Heating capacity of exhaust gas $(Q_{RDF}, kW)$ 82.75Heating capacity of hot fluid $(Q_{HF}, kW)$ 361.39Heat loss at incinerator $(Q_{Loss}, kW)$ 245.01Power consumption of absorber pump $(W_{AF}, kW_c)$ 0.23Power consumption of hot air blower $(W_{HBF}, kW_c)$ 1.31Energy efficiency of incinerator $(\eta_{ICHF}, \%)$ 52.32Hof fluid tank89Power consumption of hot fluid pump $(W_{HF}, kW_c)$ 1.89Power consumption of hot water pump $(W_{HFF}, kW_c)$ 1.88High-side pressure $(P_{HAFF}, bar gauge)$ 0.97ORC105.38Hot water temperature entering ORC $(T_{50}, {}^{\circ}C)$ 105.38Hot water temperature leaving ORC $(T_{60}, {}^{\circ}C)$ 94.65High-side pressure $(P_{HARC}, bar gauge)$ 1.70Power consumption of oil pump $(W_{OF}, kW_c)$ 1.4Low-side pressure $(P_{LORC}, bar gauge)$ 1.70Power consumption of working fluid pump $(W_{OF}, kW_c)$ 1.78Power consumption of cooling pump $(W_{CF}, kW_c)$ 1.95Power consumption of cooling tower $(W_{CF}, kW_c)$ 1.01Power of expander $(W_{ESP}, kW)$ 44.61	Enthalpy of hot fluid leaving incinerator ( $h_{3h}$ , kJ/kg)	378.85
Enthalpy of water entering absorber1 ( $h_{CW,r}$ , kJ/kg)  Heating capacity of RDF ( $Q_{RDF-S}$ , kW)  689.15  Heating capacity of exhaust gas ( $Q_{EIP}$ , kW)  82.75  Heating capacity of hot fluid ( $Q_{IIP}$ , kW)  361.39  Heat loss at incinerator ( $Q_{Lous}$ , kW)  245.01  Power consumption of absorber pump ( $W_{AP}$ , kW <sub>c</sub> )  0.23  Power consumption of hot air blower ( $W_{IIB}$ , kW <sub>c</sub> )  1.31  Energy efficiency of incinerator ( $\eta_{ICIS}$ , %)  52.32  Hot fluid tank  Power consumption of hot fluid pump ( $W_{IIP}$ , kW <sub>c</sub> )  1.89  Power consumption of hot water pump ( $W_{IIIP}$ , kW <sub>c</sub> )  1.88  High-side pressure ( $P_{ILIFIP}$ ) bar gauge)  0.97  ORC  Hot water temperature entering ORC ( $T_{34}$ , °C)  Hot water temperature leaving ORC ( $T_{65}$ , °C)  194.65  High-side pressure ( $P_{ILORC}$ ) bar gauge)  1.70  Power consumption of working fluid pump ( $W_{IP}$ , kW <sub>c</sub> )  1.78  Power consumption of working fluid pump ( $W_{P}$ , kW <sub>c</sub> )  1.78  Power consumption of cooling pump ( $W_{CP}$ , kW <sub>c</sub> )  1.95  Power consumption of cooling tower ( $W_{CP}$ , kW <sub>c</sub> )  1.01  Power of expander ( $W_{Exp}$ , kW)  44.61	Enthalpy of exhaust entering incinerator ( $h_{6e}$ , kJ/kg)	472.35
Enthalpy of water entering absorber1 ( $h_{CW,r}$ , kJ/kg)  Heating capacity of RDF ( $Q_{RDF-S}$ , kW)  689.15  Heating capacity of exhaust gas ( $Q_{EIP}$ , kW)  82.75  Heating capacity of hot fluid ( $Q_{IIP}$ , kW)  361.39  Heat loss at incinerator ( $Q_{Lous}$ , kW)  245.01  Power consumption of absorber pump ( $W_{AP}$ , kW <sub>c</sub> )  0.23  Power consumption of hot air blower ( $W_{IIB}$ , kW <sub>c</sub> )  1.31  Energy efficiency of incinerator ( $\eta_{ICIS}$ , %)  52.32  Hot fluid tank  Power consumption of hot fluid pump ( $W_{IIP}$ , kW <sub>c</sub> )  1.89  Power consumption of hot water pump ( $W_{IIIP}$ , kW <sub>c</sub> )  1.88  High-side pressure ( $P_{ILIFIP}$ ) bar gauge)  0.97  ORC  Hot water temperature entering ORC ( $T_{34}$ , °C)  Hot water temperature leaving ORC ( $T_{65}$ , °C)  194.65  High-side pressure ( $P_{ILORC}$ ) bar gauge)  1.70  Power consumption of working fluid pump ( $W_{IP}$ , kW <sub>c</sub> )  1.78  Power consumption of working fluid pump ( $W_{P}$ , kW <sub>c</sub> )  1.78  Power consumption of cooling pump ( $W_{CP}$ , kW <sub>c</sub> )  1.95  Power consumption of cooling tower ( $W_{CP}$ , kW <sub>c</sub> )  1.01  Power of expander ( $W_{Exp}$ , kW)  44.61	Enthalpy of the ambient temperature ( $h_0$ , kJ/kg)	431.18
Heating capacity of exhaust gas $(Q_{EII}, kW)$ 361.39  Heating capacity of hot fluid $(Q_{IIF}, kW)$ 361.39  Heat loss at incinerator $(Q_{Los}, kW)$ 245.01  Power consumption of absorber pump $(W_{AP}, kW_e)$ 0.23  Power consumption of hot air blower $(W_{IIB}, kW_e)$ 1.31  Energy efficiency of incinerator $(\eta_{ICII}, \%)$ 52.32  Hot fluid tank  Power consumption of hot fluid pump $(W_{IIF}, kW_e)$ 1.89  Power consumption of hot water pump $(W_{IIF}, kW_e)$ 1.88  High-side pressure $(P_{ILIFT}, bar gauge)$ 0.97  ORC  Hot water temperature entering ORC $(T_{SI}, ^{\circ}C)$ 105.38  Hot water temperature leaving ORC $(T_{SI}, ^{\circ}C)$ 94.65  High-side pressure $(P_{ILORC}, bar gauge)$ 10.41  Low-side pressure $(P_{ILORC}, bar gauge)$ 1.70  Power consumption of oil pump $(W_{OP}, kW_e)$ 1.4  Power consumption of working fluid pump $(W_{P}, kW_e)$ 1.78  Power consumption of cooling pump $(W_{CP}, kW_e)$ 1.95  Power consumption of cooling tower $(W_{CT}, kW_e)$ 1.01  Power of expander $(W_{ESP}, kW)$ 44.61	Enthalpy of water entering absorber1 ( $h_{CW,i}$ , kJ/kg)	119.71
Heating capacity of hot fluid $(Q_{HF}, kW)$ 361.39  Heat loss at incinerator $(Q_{Loss}, kW)$ 245.01  Power consumption of absorber pump $(W_{AF}, kW_c)$ 0.23  Power consumption of hot air blower $(W_{HB}, kW_c)$ 1.31  Energy efficiency of incinerator $(\eta_{ICH}, \%)$ 52.32  Hot fluid tank  Power consumption of hot fluid pump $(W_{HF}, kW_c)$ 1.89  Power consumption of hot water pump $(W_{HF}, kW_c)$ 1.88  High-side pressure $(P_{HHFT}, \text{ bar gauge})$ 0.97  ORC  Hot water temperature entering ORC $(T_{5h}, ^{\circ}C)$ 105.38  Hot water temperature leaving ORC $(T_{5h}, ^{\circ}C)$ 94.65  High-side pressure $(P_{HJORC}, \text{ bar gauge})$ 1.70  Power consumption of oil pump $(W_{OF}, kW_c)$ 1.4  Power consumption of sorking fluid pump $(W_{F}, kW_c)$ 1.78  Power consumption of cooling pump $(W_{CF}, kW_c)$ 1.95  Power consumption of cooling pump $(W_{CF}, kW_c)$ 1.01  Power of expander $(W_{Egp}, kW)$ 44.61	Heating capacity of RDF ( $Q_{RDF-3}$ , kW)	689.15
Heat loss at incinerator $(Q_{Loss}, kW)$ 245.01Power consumption of absorber pump $(W_{AP}, kW_e)$ 0.23Power consumption of hot air blower $(W_{HB}, kW_e)$ 1.31Energy efficiency of incinerator $(\eta_{ICH}, \%)$ 52.32Hot fluid tank $V_{IR}(W_{IR}, kW_e)$ 1.89Power consumption of hot fluid pump $(W_{HF}, kW_e)$ 1.88High-side pressure $(P_{ILHFT}, bar gauge)$ 0.97ORC $V_{IR}(W_{IR}, W_e)$ Hot water temperature entering ORC $(T_{Sh}, ^{\circ}C)$ 105.38Hot water temperature leaving ORC $(T_{Sh}, ^{\circ}C)$ 94.65High-side pressure $(P_{ILORC}, bar gauge)$ 1.70Power consumption of oil pump $(W_{OF}, kW_e)$ 1.4Power consumption of working fluid pump $(W_{F}, kW_e)$ 1.78Power consumption of cooling pump $(W_{CF}, kW_e)$ 1.95Power consumption of cooling tower $(W_{CF}, kW_e)$ 1.01Power of expander $(W_{Exp}, kW)$ 44.61	Heating capacity of exhaust gas $(Q_{EH}, kW)$	82.75
Power consumption of absorber pump $(W_{AP}, kW_e)$ 0.23Power consumption of hot air blower $(W_{HB}, kW_e)$ 1.31Energy efficiency of incinerator $(\eta_{ICH}, %)$ 52.32Hot fluid tankPower consumption of hot fluid pump $(W_{HF}, kW_e)$ 1.89Power consumption of hot water pump $(W_{HW}, kW_e)$ 1.88High-side pressure $(P_{HAFT}, bar gauge)$ 0.97ORCHot water temperature entering ORC $(T_{5h}, ^{\circ}C)$ 105.38Hot water temperature leaving ORC $(T_{6h}, ^{\circ}C)$ 94.65High-side pressure $(P_{LORC}, bar gauge)$ 10.41Low-side pressure $(P_{LORC}, bar gauge)$ 1.70Power consumption of oil pump $(W_{OP}, kW_e)$ 1.4Power consumption of working fluid pump $(W_{P}, kW_e)$ 1.78Power consumption of cooling pump $(W_{CP}, kW_e)$ 1.95Power consumption of cooling tower $(W_{CP}, kW_e)$ 1.01Power of expander $(W_{Exp}, kW)$ 44.61	Heating capacity of hot fluid $(Q_{HF}, kW)$	361.39
Power consumption of hot air blower $(W_{HB}, kW_e)$ 1.31  Energy efficiency of incinerator $(\eta_{ICH}, \%)$ 52.32  Hot fluid tank  Power consumption of hot fluid pump $(W_{HF}, kW_e)$ 1.89  Power consumption of hot water pump $(W_{HW}, kW_e)$ 1.88  High-side pressure $(P_{H.HFT}, \text{ bar gauge})$ 0.97  ORC  Hot water temperature entering ORC $(T_{5h}, ^{\circ}C)$ 105.38  Hot water temperature leaving ORC $(T_{6h}, ^{\circ}C)$ 94.65  High-side pressure $(P_{H.ORC}, \text{ bar gauge})$ 10.41  Low-side pressure $(P_{L.ORC}, \text{ bar gauge})$ 1.70  Power consumption of oil pump $(W_{OF}, kW_e)$ 1.4  Power consumption of working fluid pump $(W_F, kW_e)$ 1.78  Power consumption of cooling pump $(W_{CF}, kW_e)$ 1.95  Power of expander $(W_{Exp}, kW)$ 44.61	Heat loss at incinerator $(Q_{Loss}, kW)$	245.01
Energy efficiency of incinerator ( $\eta_{ICII}$ , %) 52.32  Hot fluid tank  Power consumption of hot fluid pump ( $W_{HF}$ , kW <sub>e</sub> ) 1.89  Power consumption of hot water pump ( $W_{HW}$ , kW <sub>e</sub> ) 1.88  High-side pressure ( $P_{H,HFT}$ , bar gauge) 0.97  ORC  Hot water temperature entering ORC ( $T_{5h}$ , °C) 105.38  Hot water temperature leaving ORC ( $T_{6h}$ , °C) 94.65  High-side pressure ( $P_{H,ORC}$ , bar gauge) 10.41  Low-side pressure ( $P_{L,ORC}$ , bar gauge) 1.70  Power consumption of oil pump ( $W_{OP}$ , kW <sub>e</sub> ) 1.4  Power consumption of working fluid pump ( $W_{P}$ , kW <sub>e</sub> ) 1.78  Power consumption of cooling pump ( $W_{CP}$ , kW <sub>e</sub> ) 1.95  Power consumption of cooling tower ( $W_{CT}$ , kW <sub>e</sub> ) 1.01  Power of expander ( $W_{Exp}$ , kW) 44.61	Power consumption of absorber pump $(W_{AP}, kW_c)$	0.23
Hot fluid tankPower consumption of hot fluid pump $(W_{HF}, kW_e)$ 1.89Power consumption of hot water pump $(W_{HW}, kW_e)$ 1.88High-side pressure $(P_{H,HFT}, bar gauge)$ 0.97ORCHot water temperature entering ORC $(T_{5h}, {}^{\circ}C)$ 105.38Hot water temperature leaving ORC $(T_{6h}, {}^{\circ}C)$ 94.65High-side pressure $(P_{H,ORC}, bar gauge)$ 10.41Low-side pressure $(P_{L,ORC}, bar gauge)$ 1.70Power consumption of oil pump $(W_{OP}, kW_e)$ 1.4Power consumption of working fluid pump $(W_P, kW_e)$ 1.78Power consumption of cooling pump $(W_{CP}, kW_e)$ 1.95Power consumption of cooling tower $(W_{CT}, kW_e)$ 1.01Power of expander $(W_{Exp}, kW)$ 44.61	Power consumption of hot air blower $(W_{HB}, kW_e)$	1.31
Power consumption of hot fluid pump $(W_{HF}, kW_e)$ 1.89Power consumption of hot water pump $(W_{HW}, kW_e)$ 1.88High-side pressure $(P_{H,HFT}, kW_e)$ 0.97ORCHot water temperature entering ORC $(T_{5h}, {}^{\circ}C)$ 105.38Hot water temperature leaving ORC $(T_{6h}, {}^{\circ}C)$ 94.65High-side pressure $(P_{H,ORC}, kW_e)$ 1.70Power consumption of oil pump $(W_{OP}, kW_e)$ 1.70Power consumption of working fluid pump $(W_{P}, kW_e)$ 1.78Power consumption of cooling pump $(W_{CP}, kW_e)$ 1.95Power consumption of expander $(W_{Exp}, kW)$ 44.61	Energy efficiency of incinerator (η <sub>ICH</sub> , %)	52.32
Power consumption of hot water pump $(W_{HW}, kW_c)$ 1.88  High-side pressure $(P_{H,HFT}, \text{bar gauge})$ 0.97  ORC  Hot water temperature entering ORC $(T_{5h}, {}^{\circ}\text{C})$ 105.38  Hot water temperature leaving ORC $(T_{6h}, {}^{\circ}\text{C})$ 94.65  High-side pressure $(P_{H,ORC}, \text{bar gauge})$ 10.41  Low-side pressure $(P_{L,ORC}, \text{bar gauge})$ 1.70  Power consumption of oil pump $(W_{OP}, kW_c)$ 1.4  Power consumption of working fluid pump $(W_P, kW_c)$ 1.78  Power consumption of cooling pump $(W_{CP}, kW_c)$ 1.95  Power consumption of expander $(W_{Exp}, kW)$ 44.61	Hot fluid tank	
High-side pressure $(P_{H,HFT}, \text{ bar gauge})$ 0.97ORCHot water temperature entering ORC $(T_{5h}, ^{\circ}\text{C})$ 105.38Hot water temperature leaving ORC $(T_{6h}, ^{\circ}\text{C})$ 94.65High-side pressure $(P_{H,ORC}, \text{ bar gauge})$ 10.41Low-side pressure $(P_{L,ORC}, \text{ bar gauge})$ 1.70Power consumption of oil pump $(W_{OP}, \text{kW}_e)$ 1.4Power consumption of working fluid pump $(W_{P}, \text{kW}_e)$ 1.78Power consumption of cooling pump $(W_{CP}, \text{kW}_e)$ 1.95Power consumption of expander $(W_{Exp}, \text{kW})$ 44.61	Power consumption of hot fluid pump $(W_{HF}, kW_e)$	1.89
ORCHot water temperature entering ORC $(T_{Sh}, {}^{\circ}C)$ 105.38Hot water temperature leaving ORC $(T_{Sh}, {}^{\circ}C)$ 94.65High-side pressure $(P_{H,ORC}, \text{ bar gauge})$ 10.41Low-side pressure $(P_{L,ORC}, \text{ bar gauge})$ 1.70Power consumption of oil pump $(W_{OP}, kW_e)$ 1.4Power consumption of working fluid pump $(W_P, kW_e)$ 1.78Power consumption of cooling pump $(W_{CP}, kW_e)$ 1.95Power consumption of expander $(W_{Exp}, kW)$ 44.61	Power consumption of hot water pump $(W_{HW}, kW_e)$	1.88
Hot water temperature entering ORC $(T_{Sh}, {}^{\circ}C)$ 105.38Hot water temperature leaving ORC $(T_{Sh}, {}^{\circ}C)$ 94.65High-side pressure $(P_{H,ORC}, \text{ bar gauge})$ 10.41Low-side pressure $(P_{L,ORC}, \text{ bar gauge})$ 1.70Power consumption of oil pump $(W_{OP}, kW_e)$ 1.4Power consumption of working fluid pump $(W_P, kW_e)$ 1.78Power consumption of cooling pump $(W_{CP}, kW_e)$ 1.95Power consumption of cooling tower $(W_{CT}, kW_e)$ 1.01Power of expander $(W_{Exp}, kW)$ 44.61	High-side pressure ( $P_{H,HFT}$ , bar gauge)	0.97
Hot water temperature leaving ORC ( $T_{6h}$ , °C)  High-side pressure ( $P_{H,ORC}$ , bar gauge)  Low-side pressure ( $P_{L,ORC}$ , bar gauge)  1.70  Power consumption of oil pump ( $W_{OP}$ , kW <sub>e</sub> )  1.4  Power consumption of working fluid pump ( $W_P$ , kW <sub>e</sub> )  1.78  Power consumption of cooling pump ( $W_{CP}$ , kW <sub>e</sub> )  1.95  Power consumption of cooling tower ( $W_{CT}$ , kW <sub>e</sub> )  1.01  Power of expander ( $W_{Exp}$ , kW)  44.61	ORC	
High-side pressure $(P_{H,ORC}, \text{ bar gauge})$ 10.41  Low-side pressure $(P_{L,ORC}, \text{ bar gauge})$ 1.70  Power consumption of oil pump $(W_{OP}, \text{kW}_e)$ 1.4  Power consumption of working fluid pump $(W_P, \text{kW}_e)$ 1.78  Power consumption of cooling pump $(W_{CP}, \text{kW}_e)$ 1.95  Power consumption of cooling tower $(W_{CT}, \text{kW}_e)$ 1.01  Power of expander $(W_{Exp}, \text{kW})$ 44.61	Hot water temperature entering ORC $(T_{5h}, {}^{\circ}\text{C})$	105.38
Low-side pressure $(P_{L,ORC}$ , bar gauge)1.70Power consumption of oil pump $(W_{OP}, kW_e)$ 1.4Power consumption of working fluid pump $(W_P, kW_e)$ 1.78Power consumption of cooling pump $(W_{CP}, kW_e)$ 1.95Power consumption of cooling tower $(W_{CT}, kW_e)$ 1.01Power of expander $(W_{Exp}, kW)$ 44.61	Hot water temperature leaving ORC ( $T_{6h}$ , °C)	94.65
Power consumption of oil pump $(W_{OP}, kW_e)$ 1.4Power consumption of working fluid pump $(W_P, kW_e)$ 1.78Power consumption of cooling pump $(W_{CP}, kW_e)$ 1.95Power consumption of cooling tower $(W_{CT}, kW_e)$ 1.01Power of expander $(W_{Exp}, kW)$ 44.61	High-side pressure ( $P_{H,ORC}$ , bar gauge)	10.41
Power consumption of working fluid pump $(W_P, kW_e)$ 1.78  Power consumption of cooling pump $(W_{CP}, kW_e)$ 1.95  Power consumption of cooling tower $(W_{CT}, kW_e)$ 1.01  Power of expander $(W_{Exp}, kW)$ 44.61	Low-side pressure ( $P_{L,ORC}$ , bar gauge)	1.70
Power consumption of cooling pump $(W_{CP}, kW_e)$ 1.95  Power consumption of cooling tower $(W_{CT}, kW_e)$ 1.01  Power of expander $(W_{Exp}, kW)$ 44.61	Power consumption of oil pump $(W_{OP}, kW_c)$	1.4
Power consumption of cooling tower ( $W_{CT}$ , kW <sub>e</sub> )  1.01  Power of expander ( $W_{Exp}$ , kW)  44.61	Power consumption of working fluid pump $(W_P, kW_c)$	1.78
Power of expander $(W_{Exp}, kW)$ 44.61	Power consumption of cooling pump $(W_{CP}, kW_e)$	1.95
Power of expander $(W_{Exp}, kW)$ 44.61	Power consumption of cooling tower ( $W_{CT}$ , kW <sub>e</sub> )	1.01
		44.61
	Gross power generation of ORC ( $W_{ORC,gross}$ , kW <sub>e</sub> )	23.65

Table 2. Cont.

Description	Value
Net power generation of ORC ( $W_{ORC,net}$ , kW <sub>e</sub> )	20.47
Enthalpy of hot water entering ORC ( $h_{5h}$ , kJ/kg)	441.88
Enthalpy of hot water leaving ORC ( $h_{6h}$ , kJ/kg)	396.61
Heating capacity of hot water at ORC ( $Q_{HW}$ , kW)	240.36
Energy efficiency of ORC ( $\eta_{ORC}$ , %)	8.52
Adsorption chiller	
Hot water temperature entering adsorption chiller $(T_{6h}, {}^{\circ}C)$	94.65
Hot water temperature leaving adsorption chiller $(T_{7h}, {}^{\circ}C)$	94.07
High-side pressure ( $P_{H,AD}$ , bar gauge)	-0.91
Low-side pressure ( $P_{L,AD}$ , bar gauge)	-0.99
Cooling water temperature entering adsorption chiller ( $T_{CW,AD}$ , °C)	10.48
Heating capacity of desorber $(Q_{De}, kW)$	7.73
Heating capacity of evaporator $(Q_{E1}, kW)$	4.00
Power consumption of air compressor ( $W_{AC}$ , kW <sub>e</sub> )	0.046
Coefficient of performance of adsorption chiller (COP <sub>AD</sub> , -)	0.514
Absorption chiller	
Hot water temperature entering absorption chiller $(T_{7h}, {^{\circ}C})$	94.07
Hot water temperature leaving absorption chiller $(T_{8h}, {}^{\circ}\mathbb{C})$	93.50
High-side pressure ( $P_{HAB}$ , bar gauge)	-0.92
Low-side pressure ( $P_{L,AB}$ , bar gauge)	-0.99
Cooling water temperature entering absorption chiller ( $T_{CW,AD}$ , °C)	11.86
Heating capacity of generator $(Q_G, kW)$	7.72
Heating capacity of evaporator2 ( $Q_{E2}$ , kW)	4.11
Power consumption of solution pump $(W_{SP}, kW_e)$	0.172
Coefficient of performance of absorption chiller (COP <sub>AB</sub> , -)	0.520
Drying room	
Hot water temperature entering drying room $(T_{8h}, {}^{\circ}C)$	93.50
Hot water temperature leaving drying room $(T_{9h}, {}^{\circ}C)$	90.60
Hot air temperature in drying room $(T_{HA}, {}^{\circ}\mathbb{C})$	80.00
Heating capacity of drying coil $(Q_{DC}, kW)$	38.84
Heating capacity of hot air in drying room $(Q_{DR}, kW)$	15.99
Power consumption of blower $(W_{BW}, kW_e)$	0.6
Energy efficiency of drying room ( $\eta_{DR}$ , %)	40.54
ССНР	
Net power generation of CCHP ( $W_{CCHP}$ , kW <sub>e</sub> )	11.98
Cooling capacity of CCHP ( $Q_{Cooling}$ , kW)	8.11
Heating capacity of CCHP ( $Q_{Heating}$ , kW)	15.99
Total energy generation of CCHP ( $E_{CCHP}$ , kWh)	36.08
Daily operating time ( $t_{OP,day}$ , h/d)	8
Yearly operating time ( $t_{OByear}$ , d/y)	350
Total energy generation of CCHP per year ( $E_{CCHP,year}$ , kWh/y)	101,030
Total energy generation of CCHP per lifetime ( <i>E<sub>CCHP,lifetime</sub></i> , kWh/lifetime)	2,020,592
Energy efficiency of CCHP ( $\eta_{CCHP}$ , %)	9.98
C. Com.	

formance. The correlation between the two independent variables of heat source  $(T_{HW_i})$  and heat sink  $(T_0)$  is established from the experimental hypothesis of the analysis of variance (ANOVA) in the form of a linear equation. The research results found that the thermal performances of the incinerator, organic Rankine cycle, adsorption chiller, absorption chiller, drying room, and CCHP system have a mathematical relationship, as shown in Figure 4.

Energy efficiencies of the incinerator and ORC performance curves are directly related to the Carnot cycle concept. If the heat source temperature increases, both energy efficiencies are enhanced, as presented in Figures 4(a) and 4(b). A high temperature of the heat source can generate more energy utilization from waste heat recovery of the incinerator and electricity from the ORC system.

The reverse Carnot cycle is used to describe the COPs of sorption systems. The high-temperature heat cannot generate a higher mass flow rate to produce the cool-

In addition, this research synthesized the thermal pering process at the evaporator. A concentration range of 60-65% LiBr is specifically designed for the absorption chiller, as presented in Figure 4(c). At the same time, an adsorption capacity above 16% and a pore volume range of 0.60–0.85 mL/g are used to control a hot water temperature of approximately 90-95 °C to produce a cooled water temperature of approximately 10-15 °C, as presented in Figure 4(d).

> In the case of the drying room, a high amount of heat loss from conduction and convection heat transfers increasingly reveals itself at a high level of drying air. Thus, the thermal performance of the drying system slightly decreases when the hot air temperature increases, as presented in Figure 4(e).

> The CCHP performance curve is directly driven by the ORC performance. Power energy consumes the highest heat source input to produce electricity. Thus, the sensitivity behavior of the ORC cycle greatly affects the CCHP performance, as presented in Figure 4(f).

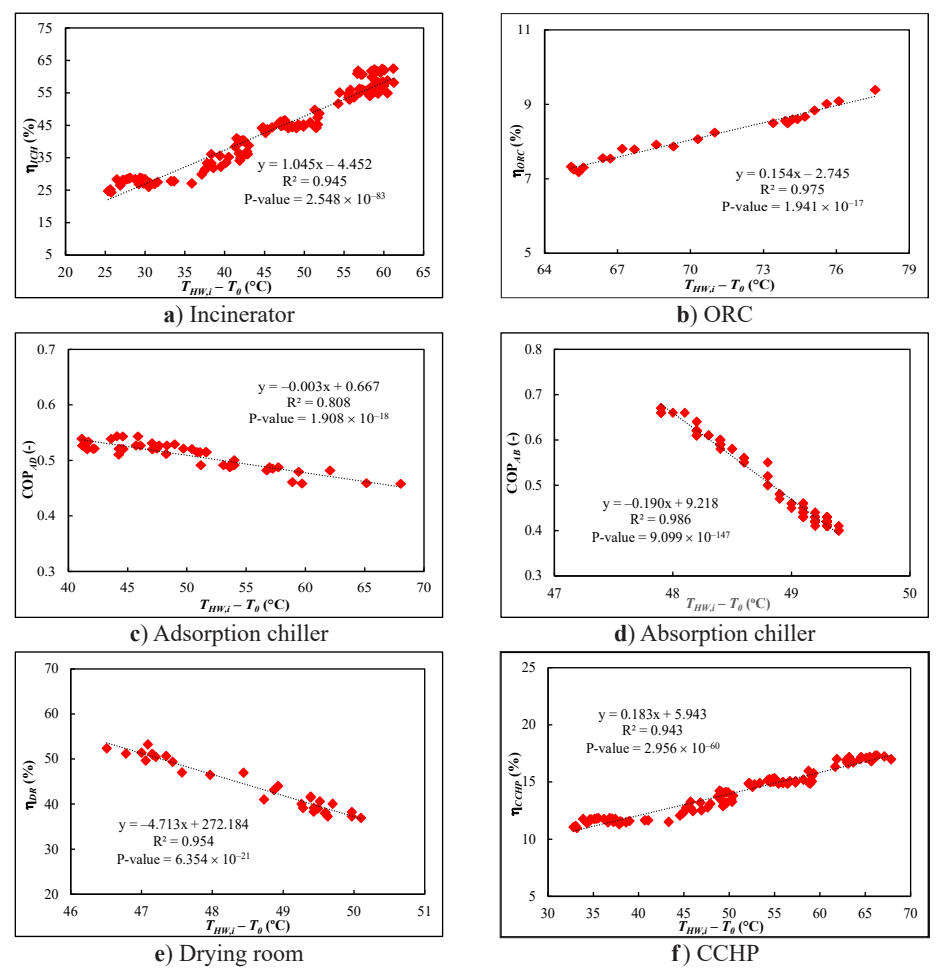


Figure 4. Performance curves of the CCHP system.

## 4.2. Construction Material from Waste Combustion Ash

The concrete block is designed according to standard dimensions, with an average weight of 7.50 kg, a width of 39 cm, a length of 19 cm, and a thickness of 7 cm. Three mixing ratios, shown in **Table 3**, are used to investigate the mix properties. The concrete blocks were tested by soaking in water for 28 days and drying in a hot air oven at 105 °C for 24 hours. The test results showed that the concrete blocks have water absorption values within the industrial product standard TIS 58-2533, which requires less than 5%. The samples for all 3 ratios had water absorption values of 0.26%, 0.37%, and 0.41%, respectively.

The compression strength test showed that the samples of the three concrete blocks have compression strengths of 41.34 kg/cm<sup>2</sup>, 31.67 kg/cm<sup>2</sup>, and 25.86 kg/cm<sup>2</sup>, respectively. All concrete blocks have compression strengths higher than the industrial product standard TIS 58-2533, which requires a minimum of 25 kg/cm<sup>2</sup>.

In addition, the concrete blocks developed from ashes of the waste combustion process have better physical characteristics (integration) compared with general concrete blocks. A very small size of combustion ash is an advantage of the coordination of cement, sand, and crushed stone. The development process of concrete blocks is illustrated in **Figure 5**.

<b>Table 3.</b> Concrete block mixing to	Table 3.	g ratio.
--	----------	----------

E	Weight	Amount	Mixing Ratio (kg)				
Experiment	(kg)	(Block)	Ash	Cement	Sand	Crushed stone	Water
1	7.50	6	0.50	1.50	2.50	2.00	1.00
2	7.50	6	0.75	1.25	2.50	2.00	1.00
3	7.50	6	1.00	1.00	2.50	2.00	1.00



Figure 5. Development of waste ash for producing concrete blocks.

#### 4.3. Economic Result

The levelized cost analysis of the waste-multigeneration system is based on a lifetime (N) of 20 y. The multigeneration system can produce a net energy (ECCHP,life

time) of 2,020,592 kWh, with a total investment value (Inv) of approximately 97,353 USD and an operating and maintenance cost (OM) of 6,434 USD/y. The levelized cost of energy (LCOE) is found to be 0.106 USD/kWh, as detailed in **Table 4**.

Table 4. Economic analysis results.

Description	Value
Building investment ( $Z_{BD}$ , USD)	6,085
Incinerator investment $(Z_{ICH}, USD)$	9,127
Hot water tank investment ( $Z_{Tank}$ , USD)	6,085
ORC system investment ( $Z_{ORC}$ , USD)	54,761
Absorption cooling system investment ( $Z_{AD}$ , USD)	4,563
Absorption cooling system investment $(Z_{AB}, USD)$	4,563
Drying room investment ( $Z_{DR}$ , USD)	6,085
Concrete blocks system investment ( $Z_{CB}$ , USD)	6,085
Total investment (Inv, USD)	97,353
Operator cost ( $OM_{Man}$ , USD/(personday))	10
Maintenance cost is 5% of total investment (OM <sub>OT</sub> , USD/y)	2,921
Operation and maintenance costs (OM, USD)	6,434
Real interest rate $(i_{Real}, \%)$ (Bank of Thailand [25])	2.50
Inflation rate ( <i>i<sub>Inflation</sub></i> , %) (Bank of Thailand <sup>[25]</sup> )	2.75
Deterioration factor (DF, %)	2.00
Lifespan (N, y)	20
Operation period per year $(t_{OT}, h/y)$	4,200
Discount rate $(r, \%)$	5.32
Net Energy Produced per Year ( $E_{CCHP,year}$ , kWh/y)	101,030
Net Energy Produced Lifetime ( $E_{CCHP.lifetime}$ , kWh/lifetime)	2,020,592
Levelized cost of energy (LCOE, USD/kWh)	0.106

## 4.4. Environmental Perspective

The environmental impact analysis is divided into 3 assessment periods: construction, operation, and decommissioning phases. The inventory results show large amounts of raw materials used in the construction phase: 13.43 tons of steel, 1.22 tons of plastic, and 0.67 tons of copper, as presented in **Table 5**. In addition, the construction period consumes 50 kWh of electricity and 500 L of diesel for transportation. During the operation period, 7,741 tons of RDF-3 fuel are used to produce a total energy output of 2,020,592 kWh over 20 years. All pollutants from air pollution, water pollution, bottom ash, and refrigerant leakage are predicted based on the CCHP testing data. Meanwhile, during the disposal period, 48.19% of the raw materials, such as steel, aluminum, copper, and brass, can be reused.

The life cycle assessment found that the 18 intermediate impacts are mostly caused by the construction process (87.16%), operation (11.94%), and disposal (0.90%),

respectively. Based on these impacts, it can be concluded that reducing the environmental impact of the WtE multigeneration system requires redesigning the engineering process in the construction phase.

Three endpoint impacts are human health (HH) of 6.76E–09 DALY, ecosystem quality (EQ) of 1.47E–11 Species·y, and resource depletion (RD) of 1.47E–05 USD. These impacts result in a single environmental score of approximately 1.51E–04 Pt (point), based on the strategic policies of Thailand and international agencies [26], as shown in **Table 6**.

Eighteen midpoint and three endpoint perspectives are explored in detail for the substances, processes, output energy, emissions, and waste. These impacts are converted into a new weighting score to analyze the benefits in the energy, economic, and environmental impacts of the energy technology from emissions trading (ET), clean development mechanism (CDM), carbon neutrality, and net zero emissions policies in Thailand [27].

Table	5.	Life	cycle	inventory.
-------	----	------	-------	------------

Description	Raw Material	Quantity	Unit
Construction phase			
Building	Steel, low-alloyed, hot rolled	1,140	kg
	Concrete	24	m <sup>3</sup>
	Steel cold rolled coil	300	kg
	Alkyd paint	50	kg
	Steel, low-alloyed	16	kg
	Glass wool	10	kg
	Sanitary ceramic	7	kg
	Gypsum fiberboard	15	kg
	PVC	3	kg
	Synthetic rubber	1	kg
	Steel hot-dip galvanized	5	kg
ORC	Copper tube	391	kg
	Alkyd paint	10	kg
	Iron and steel	230	kg
	Steel, low-alloyed, hot rolled	2,570	kg
	Stainless steel	138	kg
	Aluminum	0.5	kg
	Flat glass	0.5	kg
	R-245fa	60	kg
	Steel tube	410	kg
	Steel hot-dip galvanized	7.5	kg
	Brass	50	kg
	Glass wool	1	kg
	Synthetic rubber	1	kg
	HDPE	20	kg
	Gasket	1	kg
	Lubricants	40	kg
Incinerator	Clay	5,700	kg
	Steel, low-alloyed, hot rolled	3,700	kg
	Cast iron	85	kg
	Steel hot dip galvanized	150	kg
	Reinforcing steel	40	kg
11111-1-1-1-1-1-1-1-1-1-1-1-1-1-1-1-1-	Glass wool	2	kg
	Alkyd paint	20	kg
	Gasket	1	kg
	Sand	15	kg
	Copper	3	kg
	PVC	3	kg
	Steel cold rolled coil	1	kg
	Synthetic rubber	1	kg
Adsorption chiller	Steel, low-alloyed, hot rolled	480	kg
	Copper	100	kg
	Glass fiber reinforced plastic	12	kg
	Brass	16	kg
	Aluminum	1.5	kg

Table	5.	Cont.
-------	----	-------

460 120 12 18 1.5 403 21.78 721.2 139.8 52.99 2,200 70	kg
12 18 1.5 403 21.78 721.2 139.8 52.99 2,200	kg kg kg kg kg kg kg
18 1.5 403 21.78 721.2 139.8 52.99 2,200	kg kg kg kg kg kg kg
1.5 403 21.78 721.2 139.8 52.99 2,200	kg kg kg kg kg kg
403 21.78 721.2 139.8 52.99 2,200	kg kg kg kg kg kg
403 21.78 721.2 139.8 52.99 2,200	kg kg kg kg
21.78 721.2 139.8 52.99 2,200	kg kg kg kg
721.2 139.8 52.99 2,200	kg kg kg
139.8 52.99 2,200	kg kg
52.99 2,200	kg
2,200	
<u> </u>	
70	kg
	kg
	kg
	kg
5	kg
15	kg
285	kg
235	kg
150	kg
10	kg
130	kg
16	kg
48	kg
8	kg
3.5	kg
0.5	kg
60	kg
13	kg
11	kg
24	kg
7	kg
	kWh
500	L
	kWh
	kg
	$\frac{\text{m}^3}{\text{m}^3}$
280	m <sup>3</sup>
2.020.502	1 ****
2,020,592	kWh
	10 10 5 15 285 235 150 10 130 16 48 8 3.5 0.5 60 13 11 24

Table 5. Cont.

Description	Raw Material	Quantity	Unit
Raw material	R-245fa leak at 1 kg/y	20	kg
	Air pollution (oxygen)	25,279,654	kg
	Air pollution (carbon dioxide)	4,240	kg
	Air pollution (carbon monoxide)	2,399	kg
	Air pollution (nitrogen dioxide)	2,099	kg
	Air pollution (nitrogen monoxide)	5,097	kg
	Air pollution (sulfur dioxide)	126	kg
	Air pollution (nitrogen)	5,997	kg
	Air pollution (methane)	63	kg
	Water pollution (biological oxygen demand)	2	m <sup>3</sup>
	Water pollution (chemical oxygen demand)	5	m <sup>3</sup>
	Water pollution (nitrogen)	0.1499	$m^3$
	Water pollution (phosphorus)	0.0007	m <sup>3</sup>
	Bottom ash	499,323	kg
Decommissioning phase			
Recycle	Steel	12,813	kg
•	Aluminum	64.49	kg
	R-245fa	60	kg
	Copper	598.78	kg
	Brass	99.5	kg
Landfill	Steel	220	kg
	All plastic	473	kg
	Alkyd paint	80	kg
	Copper	69	kg
	Glass wool	23	kg
	Concrete	24	$m^3$
	Glass	7.5	kg
Transportation	Diesel	60	L

 Table 6. Assessment of single environmental indicators.

LCA impact	Mid-Point	End-Point	Normalization	Weighting Factor	Weighting Point
Climate change	1.31E-02	1.22E-08	4.95E-03	7.09E-01	8.30E-07
Ozone depletion	1.60E-09	8.48E-13	8.50E-12	1.11E+00	8.05E-08
Particulate matter formation	2.91E-06	1.83E-09	3.33E-06	1.09E+00	2.13E-07
Terrestrial acidification	1.63E-05	3.43E-12	2.87E-06	7.84E-01	3.72E-07
Freshwater eutrophication	5.08E-06	3.41E-12	8.33E-08	7.58E-01	9.28E-06
Marine eutrophication	2.61E-05	4.43E-14	3.48E-06	8.50E-01	2.19E-06
Human toxicity	2.14E-02	7.07E-08	9.20E-06	1.02E+00	3.47E-05
Terrestrial ecotoxicity	1.49E-06	8.03E-14	6.10E-09	1.11E+00	2.00E-07
Freshwater ecotoxicity	3.81E-04	2.67E-13	4.63E-06	7.58E-01	2.63E-05
Marine ecotoxicity	4.30E-04	4.73E-14	4.41E-07	8.50E-01	4.21E-05
Mineral depletion	2.21E-02	5.09E-03	9.68E-07	7.59E-01	2.35E-05
Fossil depletion	2.03E-03	9.34E-04	3.14E-05	8.32E-01	1.09E-06
Photochemical oxidant formation	3.75E-05	3.42E-11	3.24E-05	9.14E-02	6.02E-08
Ionizing radiation	6.88E-04	5.85E-12	4.98E-06	1.08E+00	1.19E-07
Agriculture land occupation	3.28E-04	2.92E-12	1.06E-05	1.00E+00	7.27E-08
Urban land occupation	6.81E-05	6.06E-13	8.50E-08	9.91E-01	1.67E-07
Natural land transformation	1.58E-06	1.41E-14	1.66E-08	9.91E-01	9.70E-06
Water depletion	9.25E-04	1.30E-11	9.78E-06	9.32E-01	2.36E-07
Single environmental score (Pt)					1.51E-04

The WtE (power, cooling, and heating) process is demonstrated by an organic Rankine cycle of 25 kW, an adsorption system of 1.5 TR (5.28 kW), an absorption chiller of 1.5 TR, a drying room of 20 kW, and an incinerator with a capacity of 200 kg/h. The CCHP system can produce 8.11 kWh of cooling, 15.99 kWh of heating, and 11.98 kWh of power, resulting in a total energy production of 36.08 kWh. The waste-to-zero (construction material) process involves developing waste ash into concrete blocks according to the Industrial Product Standard (TIS) 58-2533, with a water absorption value below 5% and a compressive strength above 25 kg/cm<sup>2</sup>. The 3E impacts are observed as an energy efficiency of 9.98%, a levelized cost of energy of 0.106 USD/kWh, and a single environmental score of 1.62E-06 Pt. The 3E perspectives of this work are slightly lower than those of the geothermal-CCHP system [24] in energy and environmental impacts at 11.62% and 0.0260 Pt, respectively. At the same time, the economic impact is higher than that of the geothermal-CCHP system at 0.069 USD/kWh.

From the study results, the development of a modified waste incinerator into a continuous waste-feeding belt system and the enhancement of the expander's efficiency in the organic Rankine cycle power generation system should be implemented. These development approaches can increase the energy efficiency of the WtEtZ system.

#### **Author Contributions**

Conceptualization, N.C.; writing-original draft preparation, C.S. and N.C.; writing—review and editing, N.C.; funding acquisition, N.C. All authors have read and agreed to the published version of the manuscript.

## **Funding**

This study is funded by the National Research Council of Thailand (NRCT) and the School of Renewable Energy and Maejo University for the project to produce and develop graduates in renewable energy for ASEAN countries for graduate students (2021).

# 5. Conclusion and Recommendations Institutional Review Board State-

Not applicable.

## **Informed Consent Statement**

Not applicable.

## **Data Availability Statement**

All data generated during this study are included in this published article.

## **Acknowledgments**

The authors thank the Thermal Design and Technology Laboratory (TDeT Lab), Chiang Mai, Thailand for their constant support for research.

## **Conflicts of Interest**

All the authors declare that there is no conflict of interest in relation to the research, authorship, and publication of this study.

characterization factor, (Unit eq/Unit)

## **Abbreviations**

CF

<b>U</b> 1	onarra communication and control of control
CFm	midpoint characterization factor, (Unit eq)
COP	coefficient of performance, (-)
CV	characterized value, (Unit eq)
DF	deterioration factor, (%)
E	energy, (kWh)
EQ	ecosystem quality, (Species(y)
h	enthalpy, (kJ/kg)
HH	human health, (DALY)
HHV	high heating value, (MJ/kg)
i	internal rate, (%)
$I_m$	single indicator, (point)
Inv	investment cost, (USD)
IP	impact, (Unit eq)
LCOE	levelized cost of energy, (USD/kWh)
LHV	low heating value, (MJ/kg)

ṁ	mass flow rate, (kg/s)	CW	cooled water
MR	mass ratio, (%wt)	CWP	cooling water pump
N	lifetime, (y)	De	desorber
NP	normalization value, (point)	DC	drying coil
NR	normalization reference, (Unit eq/y)	e	electricity
OM	operating and maintenance, (USD)	E	evaporator
PEC	production energy cost, (USD/y)	EH	exhaust gas
Q	heating capacity, (kW)	Exp	expander
r	discount rate, (%)	FC	fan coil unit
RD	resource depletion, (USD)	FG	flue gas
T	temperature, (°C, K)	H	high
W	electrical work, (kW <sub>e</sub> )	h	hot
WF	weighting factor, (-)	HB	hot air blower
WP	weighting point, (point)	HFP	hot fluid pump
X	quantity of each material, (Unit)	HF	hot fluid
Z	system cost, (USD)	HW	hot water
AB	absorption chiller	HWP	hot water pump
AD	adsorption chiller	j	impact category
CCHP	combined cooling heating and power	L	Low
DR	drying room	OP	oil pump
HFT	hot fluid tank	OT	operating
<i>ICH</i>	combined incinerator and heat	P	refrigerant pump
ORC	organic Rankine cycle	Pd	product
RDF	refuse derived fuel	X	environmental impact categories
C 1			

## Greek

η efficiency, (%)

#### Subscript

а	moist air
A	absorber
AC	air compressor
Ad	adsorber
amb	ambient
AP	absorber pump
B	boiler
С	cold
С	cultural perspective
C	condenser
CB	combustion chamber
CF	cooling fluid
CHW	chilled water
CLF	cooling fan
CT	cooling tower

## References

- [1] Energy Policy and Planning Office, Ministry of Energy, 2025. National Energy Plan. https://www.eppo.go.th/index.php/en/component/k2/item/17093 (cited 1 May 2025). (in Thai)
- [2] Navaongxay, B., Chaiyat, N., 2019. Energy and Exergy Costings of Organic Rankine Cycle Integrated With Absorption System. Applied Thermal Engineering. 152, 67–78. DOI: https://doi.org/10.1016/j.applthermaleng.2019.02.018
- [3] Karim, S., Tofiq, T., Shariati, M., et al., 2021. 4E Analyses and Multi-Objective Optimization of a Solar-Based Combined Cooling, Heating, and Power System for Residential Applications. Energy Reports. 7, 1780–1797. DOI: https://doi.org/10.1016/j.egyr.2021.03.020
- [4] Gimelli, A., Iossa, R., Karimi, A., et al., 2025. Energy-Saving and Economic Feasibility of a Battery-Integrated Combined Cooling, Heating and Power

- (CCHP) Plant Through Waste Heat Recovery for H<sub>2</sub>O-NH<sub>3</sub> Based Absorption, Power and Cooling (APC) System. Energy. 317, 134640. DOI: https://doi.org/10.1016/j.energy.2025.134640
- [5] Cho, H., Cho, Y., Jeong, J.H., 2025. Hybrid Absorption Chiller to Improve Energy Efficiency in Combined Cooling, Heating, and Power System. Applied Thermal Engineering. 272, 126440. DOI: https://doi.org/10.1016/j.applthermaleng.2025.126440
- [6] Anvari, S., Mahian, O., Taghavifar, H., et al., 2020. 4E Analysis of a Modified Multigeneration System Designed for Power, Heating/Cooling, and Water Desalination. Applied Energy. 270, 115107. DOI: https:// doi.org/10.1016/j.apenergy.2020.115107
- [7] Xu, J., Yao, Y., Yousefi, N., 2021. Optimal Prime Mover Size Determination of a CCHP System Based on 4E Analysis. Energy Reports. 7, 4376–4387. DOI: https://doi.org/10.1016/j.egyr.2021.07.028
- [8] Zhang, Y., 2025. Optimization of Combined Cooling, Heating, and Power Systems With Thermal Energy Storage Using a Modified Genetic Algorithm. Journal of Building Engineering. 107, 112780. DOI: https:// doi.org/10.1016/j.jobe.2025.112780
- [9] Du, Y., Yang, C., Wang, H., et al., 2025. Thermodynamic Analysis of a Copper-Based Chemical Looping Combustion System With Integrated Energy Storage for Combined Cooling, Heating, and Power. Energy. 328, 136540. DOI: https://doi.org/10.1016/j.energy.2025.136540
- [10] Asim, M., Kumar, R., Kanwal, A., et al., 2023. Techno-Economic Assessment of Energy and Environmental Impact of Waste-to-Energy Electricity Generation. Energy Reports. 10, 3373–3382. DOI: https://doi.org/10.1016/j.egyr.2023.09.088
- [11] Carneiro, M.L.N.M., Gomes, M.S.P., 2019. Energy, Exergy, Environmental and Economic Analysis of Hybrid Waste-to-Energy Plants. Energy Conversion and Management. 179, 397–417. DOI: https://doi. org/10.1016/j.enconman.2018.10.007
- [12] Tan, S.T., Ho, W.S., Hashim, H., et al., 2015. Energy, Economic and Environmental (3E) Analysis of Waste-to-Energy (WTE) Strategies for Municipal Solid Waste (MSW) Management in Malaysia. Energy Conversion and Management. 102, 111–120. DOI: https://doi.org/10.1016/j.enconman.2015.02.010
- [13] Bhuiyan, M.Y., Rudra, S., Sayem, A.S.M., 2025. Pyro-Gasification of Norwegian Industrial Solid Waste (ISW) for Hydrogen Production and District Heating Application: A 4-E (Energy, Exergy, Environment, and Economic) Analysis. Energy Conversion and Management: X. 27, 101068. DOI: https://doi.

- org/10.1016/j.ecmx.2025.101068
- [14] Farajollahi, M., Almasi, N., Zahedi, A., et al., 2025. Techno-Economic Analysis of a Biogas Power Plant: Moving to Sustainable Energy Supply and Green Environment Through Waste Management. Process Safety and Environmental Protection. 193, 1197–1219. DOI: https://doi.org/10.1016/j.psep.2024.11.129
- [15] Ramos, A., 2025. Integrating Waste Thermal Conversion and Lifecycle Analysis for Sustainable Energy Production: Reflecting Upon Environmental and Economic Impacts. Sustainable Energy Technologies and Assessments. 78, 104342. DOI: https://doi.org/10.1016/j.seta.2025.104342
- [16] Cunningham, P.R., Wang, L., Kane, S., et al., 2025. Lifecycle Implications and Mechanical Properties of Carbonated Biomass Ashes as Carbon-Storing Supplementary Cementitious Materials. Biomass and Bioenergy. 197, 107772. DOI: https://doi.org/10.1016/ j.biombioe.2025.107772
- [17] Aouan, B., Fadil, M., El Alouani, M., et al., 2025. Recycling Three Local Waste Materials for Optimizing the Mechanical Performance of Fly Ash-Based Geopolymer Cement: Application of a Ternary Mixture Design and Artificial Neural Networks Modeling. Sustainable Chemistry and Pharmacy. 46, 102064. DOI: https://doi.org/10.1016/j.scp.2025.102064
- [18] Carmona-Ramírez, J.D., Bedoya-Henao, C.A., Cabrera-Poloche, F.D., et al., 2025. Exploring Sustainable Construction: A Case Study on the Potential of Municipal Solid Waste Incineration Ashes as Building Materials in San Andres Island. Case Studies in Construction Materials. 22, e04351. DOI: https://doi.org/10.1016/j.cscm.2025.e04351
- [19] Chen, Z., Kumar, D., Zhu, W., et al., 2024. Simplified Framework for Efficient Utilization of Municipal Solid Waste Incinerator Bottom Ash as Construction Material via Systematic Classification and Characterization. Construction and Building Materials. 411, 134504. DOI: https://doi.org/10.1016/j.conbuildmat.2023.134504
- [20] Zhou, Y., Yu, P., Yang, H., et al., 2024. Utilization of Municipal Solid Waste Incinerator Fly Ash Under High Temperature Sintering and Alkali Excitation for Use in Cementitious Material. Journal of Building Engineering. 94, 110005. DOI: https://doi.org/10.1016/ j.jobe.2024.110005
- [21] Schafer, M.L., Clavier, K.A., Townsend, T.G., et al., 2019. Assessment of the Total Content and Leaching Behavior of Blends of Incinerator Bottom Ash and Natural Aggregates in View of Their Utilization as Road Base Construction Material. Waste Manage-

- ment. 98, 92–101. DOI: https://doi.org/10.1016/j.was-man.2019.08.012
- [22] SimaPro, 2018. SimaPro for Education (Release 8.5.2.0): Faculty Maejo University. Available from: https://simapro.com/plans/ (cited 1 May 2025).
- [23] Chaiyat, N., Wakaiyang, Y., Inthavideth, X., 2017. Enhancement Efficiency of Organic Rankine Cycle by Using Sorption System. Applied Thermal Engineering. 122, 368–379. DOI: https://doi.org/10.1016/ j.applthermaleng.2017.05.028
- [24] Chaiyat, N., Chaongew, S., Ondokmai, P., et al., 2020. Levelized Energy and Exergy Costings Per Life Cycle Assessment of a Combined Cooling, Heating, Power and Tourism System of San Kamphaeng Hot Spring, Thailand. Renewable Energy. 146, 828–842. DOI:

- https://doi.org/10.1016/j.renene.2019.07.028
- [25] Bank of Thailand, 2025. Real Interest Rate and Inflation Rate. https://www.bot.or.th/en/our-roles/monetary-policy/mpc-publication/policy-interest-rate.html (cited 1 May 2025).
- [26] Chaiyat, N., Lerdjaturanon, W., Ondokmai, P., 2021. Life Cycle Assessment of a Combined Cooling Heating and Power Generation System. Case Studies in Chemical and Environmental Engineering. 4, 100134. DOI: https://doi.org/10.1016/j.cscee.2021.100134
- [27] Department of Climate Change and Environment, Ministry of Natural Resources and Environment, 2025. Climate Change Act. https://www.dcce.go.th/ datacenter/661 (cited 1 May 2025). (in Thai)